BACHELOR ASSIGNMENT

THERMAL ENGINEERING GROUP

DETERMINATION OF PYROLYSIS REACTION KINETICS OF RAW AND TORREFIED BIOMASS

Thesis submitted for obtaining the academic degree Bachelor of Science

Alena Uhrig
Advanced Technology

7th July 2014

EXAMINATION COMMITTEE
Ir. Eddy A. Bramer
Alexander C. Louwes MSc.
Dr. Arie van Houselt

UNIVERSITY OF TWENTE.

Abstract

In this research, pyrolysis reaction kinetics of raw chips, torrefied chips and torrefied pellets of mixed waste wood have been studied. Research goals were to investigate the influence of torrefaction as well as densification on pyrolysis reaction rate, activation energy and pre-exponential factor of the Arrhenius relation. Experiments with the three materials were conducted at four temperature profiles and three particle sizes in order to investigate the maximum particle size for which the reaction is still in the kinetic regime. A cyclonic thermogravimetric analyzer, designed at the University of Twente, was used to simulate (fast) pyrolysis conditions. Results show that the maximum particle size for kinetic control is $200\,\mu$m for all three material types. For this range, the experimental trend shows that the reaction rate is larger for raw than for torrefied material, indicating a faster reaction of the former. The activation energy is lower for raw than for torrefied material. While the reaction rate is larger, the activation energy and pre-exponential factor are smaller for torrefied pellets than for torrefied chips, denoting an influence of densification on these parameters.

Contents

List of Figures 1

List of Tables 2

Terminology 3

1 Introduction 5

2 Methodology 7
- 2.1 Relevant theory . . . 7
  - 2.1.1 Biomass . . . 7
  - 2.1.2 Thermochemical Conversion of Biomass . . . 8
  - 2.1.3 Thermal Decomposition of Biomass . . . 10
  - 2.1.4 Kinetic theory . . . 15
- 2.2 Experimental . . . 21
  - 2.2.1 Experimental Set-Up . . . 21
  - 2.2.2 Experimental Procedure . . . 24

3 Results 27
- 3.1 Processing . . . 27
- 3.2 Analysis and Discussion . . . 31
  - 3.2.1 Kinetic Parameters . . . 31
  - 3.2.2 Kinetic Regime . . . 38
  - 3.2.3 Influence of Moisture Content . . . 39

4 Conclusion 42

5 Recommendations 43

6 Acknowledgements 44

References 45

7 Appendix 47
- 7.1 Indications for Quality of Experiment . . . 47
- 7.2 Linear Equations Arrhenius Plots . . . 52
- 7.3 Elemental Analysis . . . 52

List of Figures

1 The estimated use of biomass in power generation 8
2 Products of pyrolysis and torrefaction processes. 9
3 Global one-step model 11
4 Shafizadeh-Chin model 11
5 modified Broido-Shafizadeh model 12
6 Multiple Step Reaction Models 12
7 Broido model 12
8 Broido-Shafizadeh model 13
9 Koufapanos model 13
10 Di Blasi-Lanzetta model 14
11 Model including secondary Tar cracking 14
12 Model of flash pyrolysis process 15
13 Schematic Cyclonic TGA setup 22
14 Cyclonic TGA setup 23
15 Biomass decomposition: Mass vs. time graph as recorded by Labview . 25
16 Reference measurement: Mass versus time of nitrogen as recorded by Labview 26
17 MATLAB output biomass conversion 29
18 MATLAB output conversion 30
19 MATLAB output k- and c-values 30
20 Arrhenius Plot Raw chips, all particle fractions 33
21 Arrhenius Plot Torrefied Pellets, all particle fractions 34
22 Arrhenius Plot Torrefied Chips, all particle fractions 35
23 Arrhenius Plot of raw chips, torrefied pellets and torrefied chips of 0-200 μm 36
24 Comparison of moisturized and dried biomass of particle size 0-200μm . 40
25 MATLAB output biomass conversion including all measurements . . . 50
26 MATLAB output conversion 50
27 MATLAB output k- and c-values 51

List of Tables

1 Explanation of Terms . . . 3
2 Explanation of TGA components . . . 24
3 Average reaction rates (in $\frac{1}{s}$) Raw chips . . . 33
4 Average reaction rates (in $\frac{1}{s}$) Torrefied Pellets . . . 35
5 Average reaction rates (in $\frac{1}{s}$) Torrefied Chips . . . 36
6 Activation Energies . . . 37
7 Pre-exponential factors . . . 37
8 Biot and Py' numbers . . . 39
9 Comparison reaction rates (in $\frac{1}{s}$) of moisturized and dried material of all three material types of size fraction 0-200μm . . . 41
10 Activation Energies and Pre-exponential factors of dried and moisturized materials of particle size 0-200μm . . . 41
11 a values . . . 50
12 Moisturized raw . . . 52
13 Moisturized Torrefied pellets . . . 52
14 Moisturized Torrefied chips . . . 52
15 Dried material 0-200 μm . . . 52
16 Elemental analysis . . . 52

Terminology

Table 1: Explanation of Terms

Term	**Explanation**
Activation energy	Energy threshold needed to be overcome such that molecules can get close enough to react and form products
Ashes	Non-combustible residues
Char	Solid material that remains after light gases and tar have been driven out; mostly carbon
Cellulose	Most common organic compound on earth; primary structural component of cell walls in biomass; generic formula $(C_6H_{10}O_5)_n$; long polymer with high degree of polymerization and large molecular weight; has a crystalline structure
Energy density	Amount of energy stored in a system per unit volume
Hemicellulose	Component of cell wall in biomass; generic formula $(C_5H_8O_4)_n$; group of carbohydrates with branched chain structure and lower degree of polymerization; has random amorphous structure with little strength
Higher heating value (HHV)	Amount of heat released by a specific quantity, initially at room temperature, once it is combusted and the products have returned to room temperature. The vapors are condensed, such that all water is in liquid state at the end of combustion. Thus, the amount of energy needed to evaporate the water in the combustion process is retrieved. Opposing, the lower heating value (LHV) assumes all water to be in vapor phase at the end of combustion. Thus, the energy needed to evaporate the water in the combustion process is lost. In short, HHV=LHV+evaporation energy
Lignin	One of the most abundant organic polymers on earth; component of secondary cell wall of plants; varying generic formula; complex, highly branched polymer
Pre-exponential factor	Also called frequency factor, it can be regarded as the frequency at which molecular collisions happen irrespective of their energy level
Pyrolysis oil	Bio-oil; more explanation in chaper 2.1.2

Continued on next page

Table 1 – *Continued from previous page*

Term	**Explanation**
Rate constant	Frequency of successful molecular collisions in a material, enabling a reaction to happen
Residence time	Average amount of time during which a material is in a given location or condition. In this research, the material is biomass and the location a cyclonic thermogravimetric analyzer
Tar	Mixture of hydrocarbons and free carbons obtained from organic materials through pyrolysis; also referred to as condensable vapors since they can be further condensed to produce bio-oil; dark-brown, viscous and sticky liquid
Second generation bio-fuels	Produced by thermochemical conversion, they are not competing with the food supply and biodiversity as first generation biofuels (sugars, vegetable oils) do. Secondary generation bio-fuels are produced from, for example, woody crops, agricultural residues or waste.
Volatiles	Elements/compounds with lower boiling point than the remaining elements/compounds. In this research, volatiles are nitrogen, hydrogen, oxygen and water as they have a lower boiling point than carbon

1 Introduction

The shift from nuclear and fossil energy to energy production from renewable sources is inevitable as manhood eventually runs out of fossil fuels. The importance of renewable energy sources is emphasized by political bodies like the European Union. Formulating the ”20-20-20” targets, which include the reduction of greenhouse gas emissions and increasing the power production from renewable energy sources, they stimulate research in related areas all across the EU. A possible way of reducing carbon dioxide emissions in static applications like boilers, engines, furnaces and turbines is the use of pyrolysis oil. Also called bio-oil, it is a liquid produced from biomass, which can be mixed with conventional fossil oil for energy and chemistry applications and is a potential substitute for fuel oil in electricity and/or heat generation in the future. Conversion of biomass to bio-oil at or near the biomass source will reduce transportation costs and environmental concerns.

Bio-oil is produced from organic material by a process called pyrolysis, a thermochemical conversion process in which the feedstock is heated to 250-600 °C in the absence of oxygen. The biomass will decompose into a solid product, condensable gases and non-condensable gases. Flash pyrolysis, taking place at 400-600 °C, maximizes the yield of condensable gases, which can be further condensed to produce the oil-like substance. The solid part and non-condensable gases can be used to provide the heat for the process. At the moment, the quality (pH, oxygen and hydrogen content) of pyrolysis oil is a lot lower than that of fossil oil. It is highly acidic due to its organic nature and unstable over time. It ages due to slow reactions still taking place within the oil, thereby slowly altering the composition of the oil and increasing its viscosity. The higher heating value of about 20 $\frac{\mathrm{MJ}}{\mathrm{kg}}$ for a woody feedstock is much lower than the higher heating value of 45 $\frac{\mathrm{MJ}}{\mathrm{kg}}$ for fossil oil.

A number of methods aiming at the increase in quality of pyrolysis oil are currently being researched on, ranging from in-situ upgrading by the use of catalysts to downstream upgrading by chemically removing all acid content. Torrefaction as pretreatment seems to be a promising method because it removes parts of the volatile fractions. Torrefaction is a mild form of pyrolysis, roasting the feedstock at a moderate temperature of typically 200-300 °C in the absence of oxygen. During torrefaction, the biomass partly decomposes and water and part of the volatiles, amongst which are several acids, are released. It is expected that pyrolyzing this biomass, which is partly pre-decomposed and free of water and acids, will yield a better quality pyrolysis oil.

In order to test this thesis, experiments need to be conducted in existing pyrolysis reactors, which were mainly built for feeding raw biomass. It is thus essential to find out how torrefied material behaves and most importantly, if and how conversion time changes with (degree of) torrefaction. Further, it is desirable to get deeper insight in the process of producing bio-oil from torrefied biomass by pyrolysis. Here, kinetic information is of importance in order to create a kinetic model for the biomass particles. On these grounds, the aim of this bachelor assignment is to compare the chemical reaction kinetics of torrefied biomass to those of raw biomass during pyrolysis. To do so, the first research goal is to find the reaction rate, activation energy and pre-exponential factor of raw wood, torrefied wood chips and torrefied pellets of different size distributions at different temperatures. The latter have been chosen to investigate whether densification by pelletisation has an impact on the reactivity of torrefied biomass. The second research goal is to find the maximum biomass particle size for which intrinsic kinetics are still rate determining such that heat transfer limitations are prohibited.

Meng et al, who studied the effect torrefaction has on the chemistry of bio-oil produced from loblolly pine chips by fast pyrolysis, conclude that thermally treated biomass is less reactive at the same pyrolysis conditions than raw biomass. Pyle and Zaror show that, in general, kinetic control is increased when particle size is decreased. Both researches only deliver qualitative statements. In order to draw quantitative conclusions about the reaction kinetics, this research aims at finding exact numbers.

2 Methodology

This chapter provides the systematic approach to investigate the research goals. First, specific research questions are formulated, followed by delivering the essential theoretical concepts and relevant theory from which hypotheses are proposed. Then, the experimental part, including set-up and procedure, used to investigate the hypotheses, is presented.

Research questions

From the research goals, the following research questions are formulated:

- Are the reaction rates, activation energies and pre-exponential factors of raw and torrefied biomass different?
- Does densification by pelletisation of torrefied biomass yield a different reaction rate, activation energy and pre-exponential factor?
- What is the maximum particle size for a biomass particle to still be in the kinetic regime during the pyrolysis process?

Approach

In order to answer the research questions, the following approach is applied in this study. First, relevant theory is studied, including thermochemical conversion and thermal decomposition processes of biomass as well as reaction kinetics. Then, experiments using a special kind of thermogravimetric analyzer are conducted. The results are processed in MATLAB and Excel, using the mathematical relations from the theory on reaction kinetics.

2.1 Relevant theory

2.1.1 Biomass

Biomass is the term referring to organic material originating from living or recently living organisms. Mostly stemming from plants, its main representative is wood. Looking at the chemical composition, biomass is a composite material consisting primarily of cellulose, hemicelluloses and lignin, proportion and chemical structure being impacted by variety [DB08]. It can be processed to solid fuels or converted to liquid or gaseous forms for the production of heat, electric power, chemicals or fuels. Biomass is a carbon neutral energy source and therefore attractive in replacing fossil fuels in the future [SGKP11]. The estimated increase in the use of biomass in power generation is shown in figure 1. The y-axis shows the amount of energy (in exajoules, 10^{18} Joules) and the x-axis the years from 1860 to 2060. As one can see, the biomass use will increase from zero in the 1990's to around 200 exajoules in 2060. In 2060, it will be on the same level as gas, both being the leading feedstock for power generation. Thus, biomass is becoming the most attractive renewable energy source for power generation in the future.

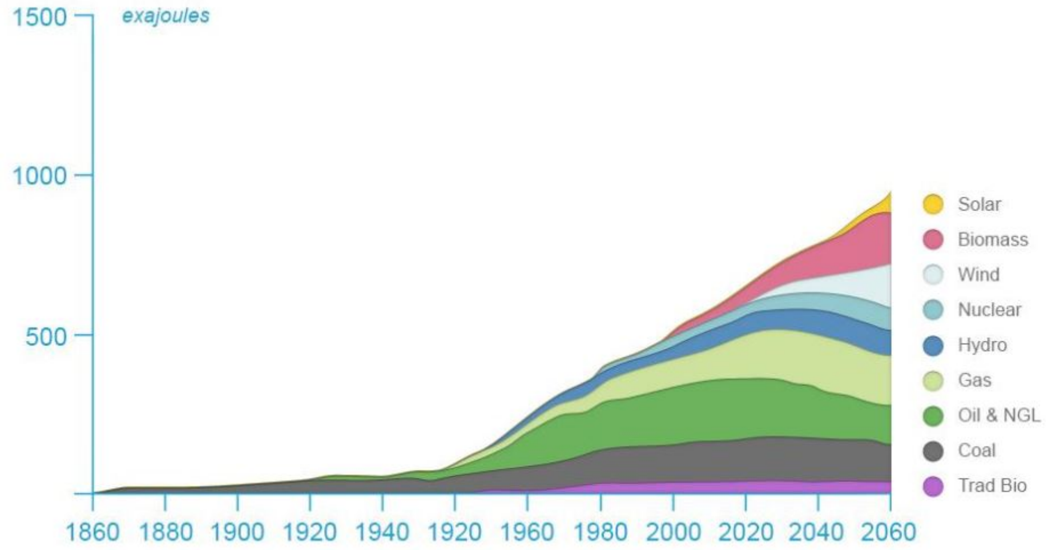

Figure 1: The estimated use of biomass in power generation [Ker13]. In the future, biomass is expected to be one of the largest feedstocks in energy generation from renewable sources.

2.1.2 Thermochemical Conversion of Biomass

Conversion of biomass to bio-fuels can be achieved via processes classified as thermal, chemical and biochemical methods, or a combination of these. In this research, thermochemical processes, more precisely pyrolysis and torrefaction, are applied. In thermochemical conversion, biomass is transformed to obtain thermal energy or chemical energy in a different physical state. Thus, the thermally treated biomass has altered physical and chemical properties. After the conversion, the product has a higher energy density than untreated biomass [NRVP12].

Pyrolysis

Pyrolysis is the endothermic process of treating biomass at elevated temperatures in the range of 225-600 °C without the supply of oxygen. During this process, decomposition of biomass into char, non condensable gases and condensable vapors takes place. The latter are further condensed to produce the desired bio-oil. Flash pyrolysis, also executed in this assignment, is performed at 450-550°C and aims at maximizing the yield of the liquid products. Advantage of pyrolysis is the production of a renewable fuel for power generation in boilers, engines, gasifiers and turbines. The oil has a higher energy density and higher carbon, less hydrogen and oxygen content than the untreated material. Further, decoupling of liquid fuel production from use in location and time is possible. The bio-oil features less rotting than raw biomass. Rotting biomass produces methane and looses carbon (to the soil). Separation of minerals on the fuel production site is possible. The minerals can be recycled to the soil as nutrient source [NRVP12].

Pyrolysis Oil

The production of bio-oil from biomass by pyrolysis is a carbon neutral process. Pyrolysis oil is classified as second generation bio-fuel. The oil is of dark brown color, as shown in figure 2 (left), containing a low amount of ash and having a (volumetric) energy density about ten times higher than the original biomass. It is not miscible with hydrocarbons. The remaining moisture content amounts to about 25%. The higher heating value (HHV) of pyrolysis oil is about 17 $\frac{\mathrm{MJ}}{\mathrm{l}}$ and the pH about 2.5, originating from the organic acids produced from the decomposition process. Elemental analysis gives average fractions for C, H, O and N of about 56%, 6%, 38% and 0-0.1% respectively [CG11].

Figure 2: Products of pyrolysis and torrefaction processes. *left*: Pyrolysis bio-oil [Bra13]. *right*: torrefied pellets with residence time of 60 minutes at temperatures 200°C, 250°C and 300°C, respectively [Nac].

Torrefaction

Torrefaction is a mild form of pyrolysis, occurring at a temperature range of 225-300 °C. Wooden pellets to which torrefaction at three different temperatures (200°C, 250°C and 300°C) has been applied for 60 minutes are shown in figure 2 (right). Compared to (flash) pyrolysis, a lot less liquid, a lot more solid and slightly less gaseous products are formed. In contrast to untreated wood, torrefied wood is hydrophobic, has better grindability and less acid content. The torrefaction product has a lower oxygen and higher carbon content, which results in an increased higher heating value [MPTP12]. The exact HHV depends on the severity of torrefaction. As example, torrefying corncob for 60 minutes at a temperature of 275°C increases the HHV from 14.85 to 17.09 $\frac{\mathrm{MJ}}{\mathrm{kg}}$ [ZZC$^+$13].

2.1.3 Thermal Decomposition of Biomass

The pyrolysis process takes place at elevated temperatures, which cause the biomass to decompose into the final products char, tar and gases. The overall decomposition process is highly complex due to the diverse composition of wood. First, the free moisture in the solid evaporates, then more unstable polymers degrade. With increasing temperature, the more refractory components start decomposing and volatiles are released. During primary decomposition, i.e. 200-400 °C, solid char residue is formed [WCL11]. Looking at the components cellulose, hemicelluloses and lignin only, three zones can be distinguished in weight loss curves. Hemicellulose, the most reactive compound, decomposes in the temperature range of 225-325 °C, cellulose at 325-375 °C and lignin over the entire temperature range of 250-500 °C [DB08].

For this research this means that during torrefaction, hemicellulose decomposes, cellulose and lignin partially decompose and the moisture content is mostly removed by evaporation. Some organic acids (e.g. acetic acid) are driven off from the biomass by the hemicellulose decomposition and oxygen is lost in form of water, carbon dioxide and carbon monoxide. All of this causes the oxygen-carbon ratio of biomass to decrease. Thus, bio-oils produced from torrefied biomass have an improved oxygen-to-carbon ratio compared to raw biomass. Removing the thermally-reactive components through the loss of volatiles during torrefaction yields a higher concentration of biomass in thermally non-reactive carbon. Thus, thermally treated wood features less reactivity at the same pyrolysis conditions than raw biomass, increasing its thermal resistance [MPTP12].

Reaction Models

As mentioned before, the decomposition of biomass is a complex processes as many reactions take place in parallel and or series, involving a large variety of components. Simplified models are used since modeling all reactions is impossible. Different approaches are presented in literature, ranging from single-step global mechanisms over single step independent reaction models to multi step mechanisms via the formation of intermediates. In order to investigate the research goal of comparing reaction rates of raw and torrefied biomass, it is essential to identify the reaction model which best suits the pyrolysis process applied in this research.

Single Step Global Reaction Model

The single step reaction model follows a first order rate law with global activation energy and reaction rate k. This scheme, shown in figure 3, models the devolatilization process, taking only the end products (char, volatiles) into consideration.

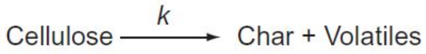

Figure 3: Global one-step model
[NRVP12]

Single Step Independent Reaction Models

These models involve single step, concurrent reactions into multiple final products. Not influencing each other, the single, independent and irreversible reactions are modeled by individual reaction rates.

Shafizadeh-Chin

This model describes the biomass degeneration as direct conversion into the final products gas, tar and char without the formation of intermediate products as shown in figure 4. The individual reaction rates are given by k_1, k_2 and k_3, respectively. The reactions are all endothermic, their rates being represented as first order in mass and with an Arrhenius type of temperature dependence.

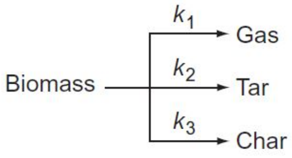

Figure 4: Shafizadeh-Chin model
[NRVP12]

Modified Broido-Shafizadeh

A modification of the more complicated Broido-Shafizadeh model, which is shown below, describes the cellulose decomposition of biomass into the products tar as well as char and gases, see figure 5. The activation reaction has been omitted, since this step is not rate limiting in the conversion of cellulose. The individual reaction rates are given by k_1 and k_2, respectively.

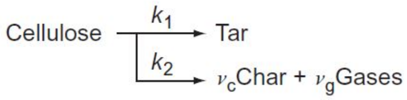

Figure 5: modified Broido-Shafizadeh model
[NRVP12]

Multi-step Models

These models describe the decomposition process as multiple reactions, via the formation of intermediate products, as shown in figure 6. The reactions can be consecutive (left), individually characterized by the reaction rates k_1, k_2 and k_3 or overlapping (right), described by the reaction rates $k_1, k_1 + k_2$ and $k_2 + k_3$, respectively.

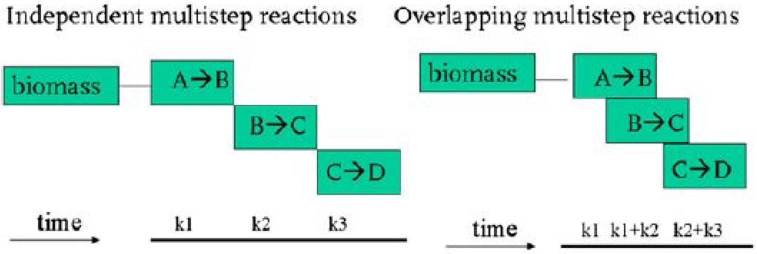

Figure 6: Multiple Step Reaction Models
[SGKP11]

Broido

Broido proposed a model, shown in figure 7, involving the irreversible formation of an intermediate, active form of cellulose (reaction rate k_{ac}). The intermediate further decomposes during competitive reactions into char (reaction rate k_{Ca}) and volatile tars (reaction rate k_{tar}). The former reacts further to form successive chars and volatiles in two consecutive reactions described by reaction rates k_{Cb} and k_{Cc}, respectively.

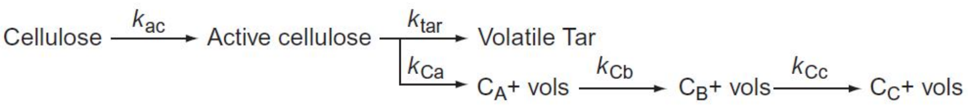

Figure 7: Broido model
[NRVP12]

Broido-Shafizadeh

The Broido-Shafizadeh model, displayed in figure 8, is a simplified form of the Broido reaction model described above. Being based on the formation of an intermediate product converted to condensable vapors (bio-oil), chars and gases, the subsequent conversion of the char product is no longer taken into account.

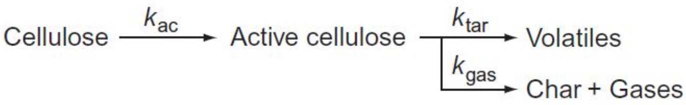

Figure 8: Broido-Shafizadeh model
[NRVP12]

Koufopanos

The Koufopanos model is based on the assumption that the components hemicellulose, cellulose and lignin convert at different rates without any interaction with other components. Therefore, the reactions of cellulose, hemicelluloses and lignin can be modeled independently. Here, more information about the intermediate step, after which product gases and volatiles as well as char are formed in different reactions, is provided. In the Koufopanos model, shown in figure 9, each individual reaction takes place according to the Broido-Shafizadeh model, the only exemption being the link of the formation of tar and non-condensable gases.

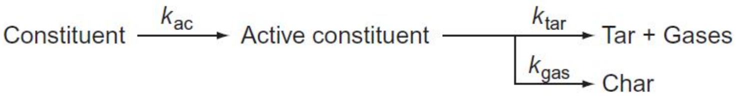

Figure 9: Koufapanos model
[NRVP12]

Di Blasi-Lanzetta

Di Blasi and Lanzetta established a model for the pyrolysis of hemicellulose, consisting of two competitive reactions, as displayed in figure 10. Hemicellulose decomposition yields volatiles and an intermediate product in reactions described by rate constants k_2 and k_1, respectively. The latter is further converted to char and additional volatiles by cellulose decomposition in reactions characterized by reaction rates k_3 and k_4, respectively.

Figure 10: Di Blasi-Lanzetta model
[NRVP12]

Di Blasi

Next to primary reactions as in the model of Shafizadeh-Chin, the model of Di Blasi in figure 11 takes into account secondary tar cracking into lighter gases or tar (reaction rates k_4 and k_5, respectively).

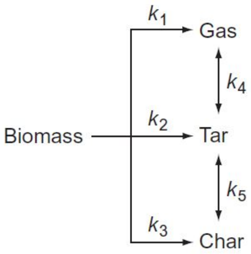

Figure 11: Model including secondary Tar cracking
[NRVP12]

Choosing the correct Model

This research aims at finding the pyrolysis reaction rates of raw and torrefied biomass. Different models about the thermal decomposition of biomass are presented above. The appropriate model should give the reaction rates of char, tar and gas formation, from which the overall reaction rate can be determined. The model needs to include all parameters necessary for modeling the (flash) pyrolysis process while omitting redundant variables or unfamiliar information not required for this work.

The single step global reaction model quantifies only the reduction in mass of the solid material, thus, provides information on the reaction time of the whole biomass conversion process. Despite the simplicity of the model, it is limited by assuming a fixed mass ratio between pyrolysis products, preventing the prediction of product yields based on process conditions. This model does not deliver information about the portion of the single end products and does not provide the flexibility to consider the variation of constituents within more complex structures such as biomass [WCL11]. Therefore, the single step global reaction model is not suitable for this research.

The models of Broido, Di Blasi and Di Blasi-Lanzetta are the most detailed for biomass decomposition. They are of limited practical use since this research aims at finding the single reaction rates for char, tar and gas formation only. Modeling activation steps or intermediates makes the process too complicated since limited knowledge on these exist.

The model of Koufopanos is not based on a specific set of experiments but rather relies upon a re-examination of literature data. It exhibits an increase in the degree of complexity of reactions since more intermediate and final products are introduced, each requiring quantification of reaction rates.

Both the Broido-Shafizadeh and Shafizadeh-Chin model treat biomass as a homogeneous material, not allowing for variations between various biomass feed materials unless the specific reaction parameters of each type are obtained individually. Still, the Shafizadeh-Chin model provides the most practical approach since it gives three individual reaction rates for the formation of gases, tar and char in the pyrolysis process. In this research, these are summed up to find the overall reaction rate. Thus, all relevant parameters are taken into account, omitting information that is not essential. A descriptive picture of the pyrolysis process according to Shafizadeh-Chin is shown in figure 12.

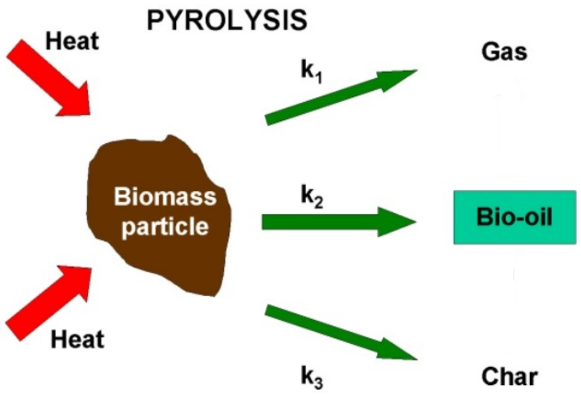

Figure 12: Model of flash pyrolysis process [Bra13]. As heat is applied to the biomass particles during pyrolysis, these decompose into gas, bio-oil and char in reactions described by reaction rates k_1, k_2 and k_3, respectively.

2.1.4 Kinetic theory

This part contains the approaches and mathematical expressions relevant for determining the kinetic parameters, namely reaction rates, activation energies and pre-exponential factors of raw and torrefied biomass. Further, mathematical relations, used to validate whether particles sizes are sufficiently small enough for intrinsic kinetics to determine the reaction, are provided.

Reaction kinetics

Kinetic information is essential to understand the mechanics of thermal processes with the objective to find a mathematical expression relating temperature, conversion and time. In this research, reaction kinetics given by [PBVG09] are applied to study the decomposition of the different forms of biomass. The goal is to find the activation energy, pre-exponential factor and the rate constant at different temperatures. Since gas phase residence times are assured to be short, at high temperatures, secondary cracking of the vapors can be disregarded and thus, the primary kinetic constant can be determined from measuring the change in weight over time [BB07].

At constant pressure, the rate of thermal processes is a function of temperature (T) and extend of conversion (α), which can be determined from mass-loss experiments:

$$\alpha = \frac{m_i - m_T}{m_i - m_f} \tag{1}$$

Where

m_i	initial mass	[kg]
m_T	mass at temperature T	[kg]
m_f	final mass	[kg]

From the model of the (flash) pyrolysis process, see figure 12, it can be deduced that all primary cracking reactions of biomass decomposition are first order in the remaining biomass [BB07], the rate equation being

$$\frac{d\alpha}{dt} = k(T)f(\alpha) \tag{2}$$

Where *k(T)* is the rate constant and f(α) the reaction model.

The rate constant and thus, temperature dependence, is universally described by the Arrhenius equation:

$$k(T) = A \cdot \exp\left(-\frac{E_a}{RT}\right) \tag{3}$$

Where

A	pre-exponential factor	$[\frac{1}{s}]$
E_a	activation energy	$[\frac{J}{mol}]$
R	universal gas constant	$[\frac{J}{mol \cdot K}]$
T	temperature	[K]

Note that the exponential term is the fraction of collisions that possess enough kinetic energy to initiate a reaction [WCL11].

For a first order reaction scheme, the biomass decomposition rate constant *k(T)* is the sum of each individual primary cracking constant of char, tar, volatiles (k_1, k_2, k_3) [BB07].

$$k(T) = k_1 + k_2 + k_3 \tag{4}$$

For thermal degradation of polymers, as it is the case in decomposition of biomass, the mathematical form of the reaction model is given by

$$f(\alpha) = (1-\alpha)^n \tag{5}$$

This equation shows that the reaction rate is proportional to the fraction of unreacted substance raised to a certain exponent n, denoting the reaction order [WCL11]. The integral form of the reaction model can be found by integrating $\frac{\mathrm{d}\alpha}{\mathrm{f}(\alpha)}$ from zero to α. For the reaction model in equation (5) and n=1, this yields

$$g(\alpha) = \int_0^\alpha \frac{d\alpha}{1-\alpha} = -\ln(1-\alpha) \tag{6}$$

Inserting experimental values of α into $g(\alpha)$ and plotting $g(\alpha)$ against time should result in a straight line with slope given by the rate constant at a given temperature *k(T)*. The values of A and E_a can be determined from the intercept and slope of the graph of $\ln(k(T))$ versus $\frac{1}{\mathrm{T}}$ by using the logarithmic form of the Arrhenius equation in (3).

The way according to which the reaction behavior of biomass changes when pre-torrefied has been explained in the chapter 2.1.3 about thermal decomposition of biomass: thermally treated wood is expected to be less reactive at the same pyrolysis conditions than untreated biomass. Less reactive means that the reaction time (in s) increases and thus the reaction rate (in $\frac{1}{s}$) decreases. The following paragraph provides expectations that can be formulated from the mathematical expressions for reaction kinetics treated above.

Assuming the same initial mass, the difference $\mathrm{m_i} - \mathrm{m_f}$ in equation (1) will be smaller for raw biomass since less carbon content remains relative to the initial mass and carbon has a larger density than the remaining components. This results in a larger value for the extend of conversion, α, given in equation (1), which on the other hand leads to a smaller f(α). For larger values of α, g(α), in equations (5) and (6) respectively, will also be larger and thus, the slope of g(α) versus time will be steeper. Therefore, the slope, which represents the reaction rate *k(T)*, will be larger for a raw biomass feed than for torrefied biomass. Looking at the Arrhenius relation, a larger reaction rate requires either the pre-exponential factor A to be larger or the activation energy E_a to be smaller for raw biomass. These expectations are consistent with [MPTP12], who claim that the thermal resistance of torrefied wood is higher than that of raw wood, indicating a slower reaction time and higher activation energy of the former.

Kinetic Regime

In order for the intrinsic kinetics to be the rate determining step, the rate of heat transfer to and within the particle needs to be fast compared to the reaction rate, such that no temperature gradient is present in the particles. In this way, the solid temperature will be the same as the surrounding temperature. In order to meet these requirements, the reaction time as well as the Biot and external Pyrolysis numbers need to be studied [PPJ06]. In order to be in the kinetic regime, the reaction time should not be a function of particle size but rather should not change when particle size is varied.

The Biot number, which is the ratio between heat convection at the surface of the particles and heat conduction within the particles, is given by [CG11]

$$Bi = \frac{h \cdot L_c}{k} \tag{7}$$

Where

h	external heat transfer coefficient	$[\frac{\mathrm{W}}{\mathrm{m^2 \cdot K}}]$
L_c	characteristic length	$[m]$
k	thermal conductivity of particle	$[\frac{W}{m \cdot K}]$

Assuming spherical particles, the characteristic length is

$$L_{c,spherical\ particle} = \frac{V}{A_s} = \frac{\frac{4}{3}\pi r^3}{4\pi r^2} = \frac{1}{3}r \tag{8}$$

Where r is the radius of the particle in meters.

In terms of particle diameter, the expression for the characteristic length becomes

$$L_{c,spherical\ particle} = \frac{1}{6}d \tag{9}$$

And thus the Biot number is given by

$$Biot_{spherical\ particle} = \frac{h \cdot d}{6 \cdot k} \tag{10}$$

Assuming cylindrical particles, the characteristic length is

$$L_{c,cylindrical\ particle} = \frac{V}{A_s} = \frac{\pi r^2 l}{2\pi r l + 2\pi r^2} = \frac{rl}{2(l+r)} \tag{11}$$

In terms of diameter, this becomes

$$L_{c,cylindrical\ particle} = \frac{dl}{2(2l+d)} \tag{12}$$

And thus the Biot number is given by

$$Biot_{cylindrical\ particle} = \frac{h}{k} \cdot \frac{dl}{2(2l+d)} \tag{13}$$

The external Pyrolysis, or Py' number, which gives the ratio between heat convection and reaction rate of a particle [PPJ06], is given by

$$Py^{'} = \frac{h}{k \cdot \rho \cdot c_p \cdot L_c} \tag{14}$$

Where

ρ	density of biomass particle	$[\frac{kg}{m^3}]$
c_p	specific heat of particle	$[\frac{J}{kg \cdot K}]$

For spherical particles, this yields

$$Py^{'}_{spherical\ particles} = \frac{6h}{k \cdot \rho \cdot c_p \cdot d} \tag{15}$$

For cylindrical particles, this yields

$$Py^{'}_{cylindrical\ particles} = \frac{h}{k \cdot \rho \cdot c_p} \cdot \frac{2(2l+d)}{dl} \tag{16}$$

A Biot number much smaller than one represents a thermally-thin regime, meaning that heat conduction within the particle is a lot faster than heat convection to the particle. For Py' numbers much larger than unity, heat convection to the particle is a lot faster than the chemical reactions taking place. Both requirements need to be met

in order for the reaction to be purely controlled by kinetics, prohibiting heat transfer limitations [PPJ06].
The cyclonic TGA setup, see chapter 2.2.1, ensures a good heat transfer, featuring a heat transfer coefficient of around $550\frac{\mathrm{W}}{\mathrm{m}^2\cdot\mathrm{K}}$ [Vis05]. Thus, in order for no temperature gradients to be present in the particles, the limiting parameter is the maximum particle size.

2.2 Experimental

Expectations

From theory, the following expectations are formulated regarding the research questions:

Compared to raw biomass, torrefied biomass features

- a lower reaction rate than raw biomass (higher reaction time)
- a lower pre-exponential factor
- a higher activation energy

In order to prove or refute these expectations, experiments are conducted. In the following chapter, the experimental set-up, procedure and program are provided.

2.2.1 Experimental Set-Up

Thermogravimetric Analysis (TGA)

Since pyrolysis is an endothermic process, a substantial heat input is necessary in order to raise the biomass to the reaction temperature [Bri12]. In thermogravimetry, a scale continuously measures the mass of a material as a function of temperature or time while ensuring a controlled temperature in a controlled atmosphere. In this research, the mass will be measured as a function of time only, keeping the temperature of the single measurements constant. Thus, isothermal conditions are applied. The drawback of conventional TGA devices is a limited heat transfer rate. Since it is essential for this research to decouple kinetics from any other heat induced reactions, high heat transfer rates in the range of $500\frac{W}{m^2 \cdot K}$ are needed. Therefore, a special kind of TGA, a device called Cyclonic TGA, is used.

Cyclonic TGA

The cyclonic TGA provides, compared to conventional TGA devices, an enhanced heat transfer rate to the reacting particles, decoupling kinetics and making flash pyrolysis conditions possible. Process demands of the latter are

- High heating rates of the biomass particles to prevent char formation
- Short vapor residence times of ≤ 2 seconds to minimize secondary reactions
- Rapid cooling of the vapors such that one liquid product is produced and cracking of the condensable products is prevented

The process demands are met by the special design of the cyclonic device, see figure 13, which consists of the upper cylindrical part of a cyclone, with a batch wise type of operation. In this way, the solid particles stay in the reactor until they are completely converted. Thus, an infinite residence time for solid particles is guaranteed. The carrier gas nitrogen is introduced in tangential direction and is, along with gaseous products, able to leave the reactor through an exit pipe in the center of the reactor, creating a swirling motion of the gases. The gas residence time is kept small, below one second, to avoid secondary cracking of primary products. Controlled biomass feeding is achieved by filling the particles in a balloon and injecting them in the reaction chamber by a pulse of nitrogen, using a pressurized gun. After injection, the particles swirl along the reactor wall because of the force exerted by the swirling motion of the gases. Being in close contact with the wall and surrounding gases, a high heat transfer rate to the reacting particles is assured [BB07]. The electric oven surrounding the reaction chamber provides the necessary heat and the sensitive balance on which the chamber is mounted, continuously measures the mass decline. Thermocouples (TI) continuously measure the temperature. They are connected to the oven, such that the temperature is regulated by the temperature control (TC) when it is above or below the desired value. The condensable gases could be condensed using a liquid cool spray to produce the pyrolysis oil. However, this installation is not yet in place.

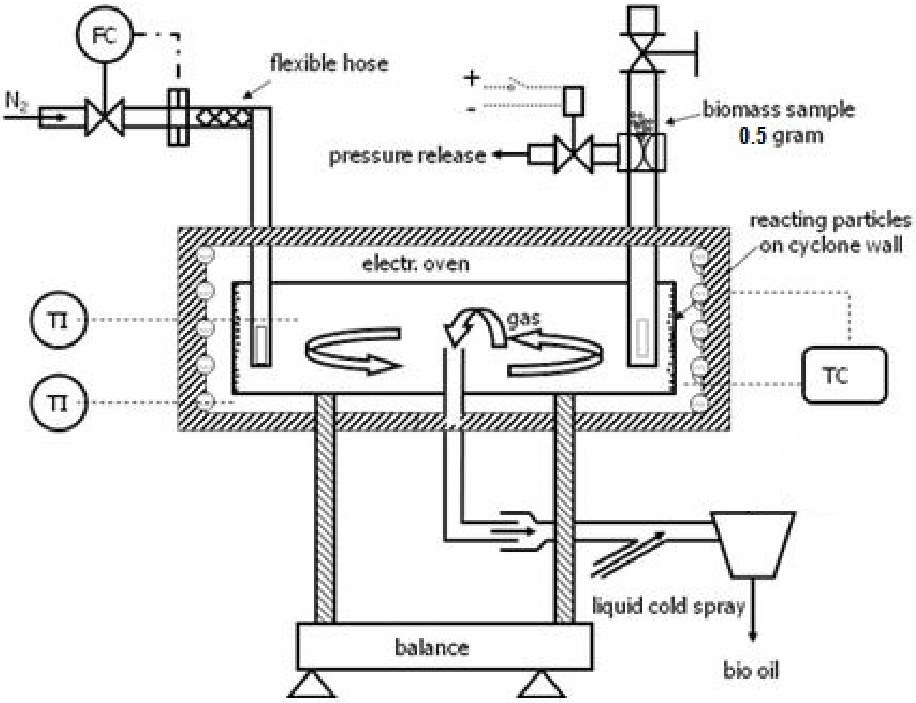

Figure 13: Schematic Cyclonic TGA setup
[BB07]

The set-up, as it looks in practice, is shown in figure 14. Table 2 lists and explains the components of the TGA.

Figure 14: Cyclonic TGA setup. The left side shows the set-up how it is used in experiments, protected by the band heater (white). On the right, the device as it looks from the inside, is shown.

Table 2: Explanation of TGA components

Number	**Component**	**Explanation**
1	Gun	Small vessel charged with inert gas (N_2) for pulsed sample injection
2	Balloon	Inflatable for controlled sample injection
3	Main valve	Prevents hot gases to escape through balloon when gun is dismantled
4	Nitrogen inlet	Supplies nitrogen to reaction chamber
5	Thermocouple	Measures the temperature; connected to oven, which, using an on/off mechanism, regulates the temperature at the desired level
6	TGA outlet	Serves as exit for gases and ashes
7	Ventilation system	Ensures proper ventilation
8	Nitrogen preheater	Heats the nitrogen to the desired temperature before it enters the reaction chamber
9	Cyclonic Reaction Chamber	Heart of the Cyclonic TGA; here, the biomass decomposition takes place

2.2.2 Experimental Procedure

Sample Preparation

Before executing experiments, the biomass samples need to be prepared. This requires the following:

1. Grinding the material
2. Sieving the material to the desired fractions
3. Weighing the mass for the single experiments

Execution

The experimental procedure for the cyclonic TGA is as follows.

1. Setting the oven to the desired temperature (it might take up to one hour for the oven to reach high temperatures)
2. Setting the pressure for the balloon as well as for the TGA and gun to the desired level

3. Switching the gas from air to nitrogen
4. Inflation of the balloon
5. Insertion of the sample into the balloon using a funnel
6. Pressurizing the gun
7. Opening the main valve
8. Checking whether nothing is caught up with any rigid support
9. Running the computer program Labview
10. Checking whether the system is stable around zero
11. Opening electromagnetic valve; this causes the gun to unload, the balloon to deflate and thus the sample to be injected into the reaction chamber
12. Recording the change in mass over time using Labview (it is advisable to let the program run for approximately 30 seconds to ensure that full conversion occured). Figure 15 shows an example of a mass versus time graph as recorded by Labview
13. After finishing the measurement, cleaning of the TGA is required by blowing controlled puffs of air through the device. This makes sure that no unreacted material is left in the reactor, which can influence subsequent measurements.

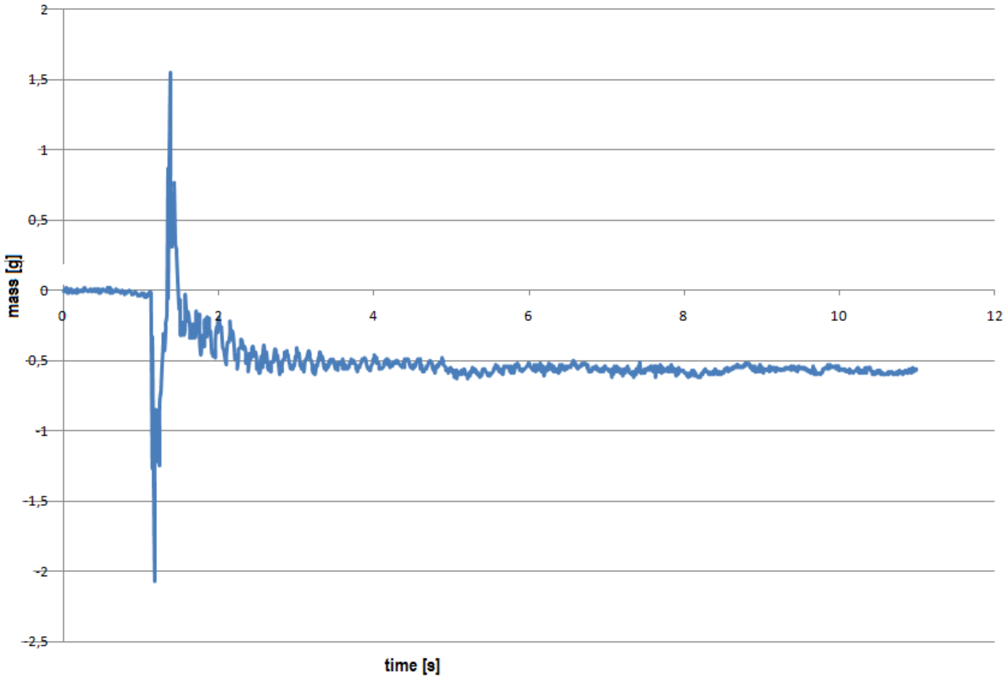

Figure 15: Biomass decomposition: Mass vs. time graph as recorded by Labview

Note that, in order to calculate the k values only from the mass loss of biomass, reference measurements need to be made. To do so, the procedure is as described above, leaving out the sample insertion. In this way, the mass of the nitrogen is recorded. Figure 16 shows an example of a mass (nitrogen only) versus time graph as recorded by Labview.

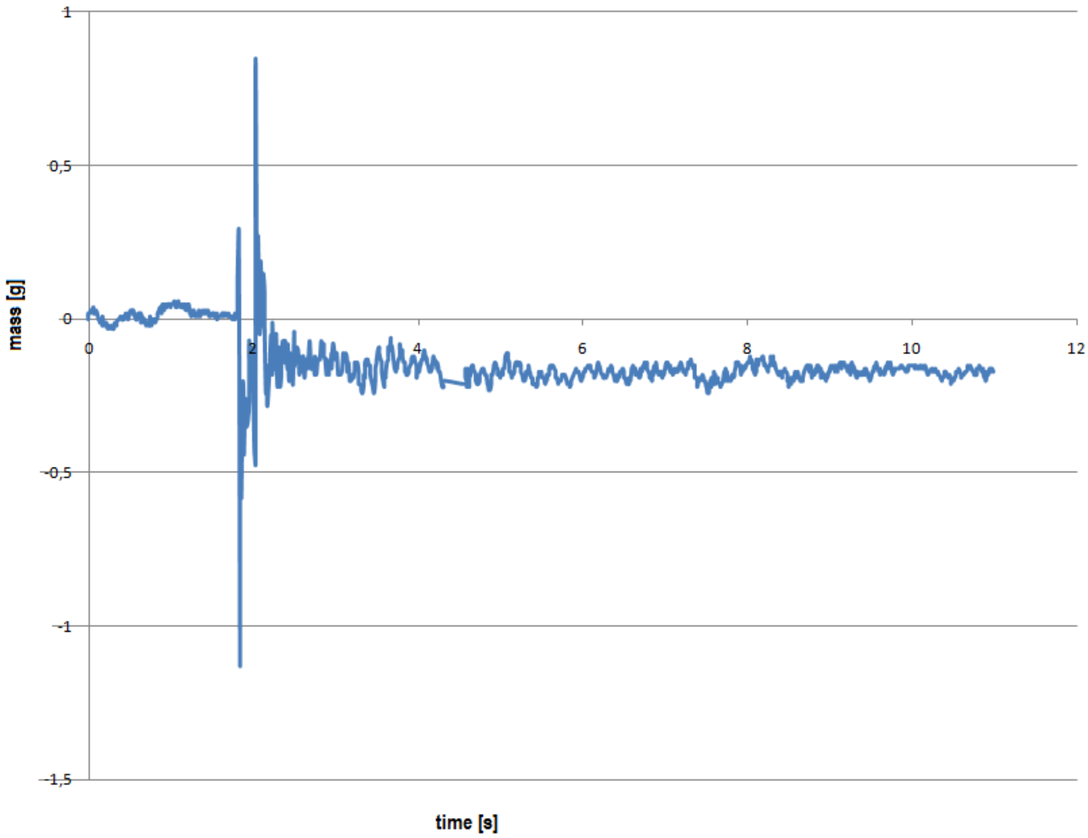

Figure 16: Reference measurement: Mass versus time of nitrogen as recorded by Labview

Experimental Test Program

In order to answer the research question on whether torrefaction yields a different reaction rate, activation energy and pre-exponential factor, experiments were done with raw and torrefied biomass. The latter was further divided into torrefied chips and pellets to test whether densification by pelletisation has an influence on the kinetic parameters. All three feedstocks originated from mixed waste wood. In order to find out the kinetic parameters, measurements at multiple temperatures are necessary. Thus, four different temperatures were used: 475°C, 500°C, 525°C and 550°C. The tolerance for each temperature was ±1°C. Investigating the research question on the maximum particle size that can be used in order for the intrinsic kinetics to be rate determining, different particle fractions were used: $0 - 200\,\mu$m, $200 - 500\,\mu$m and $500 - 800\,\mu$m. The weight of each sample used was $0.5\,g \pm 0.01$. Each condition was tested eight to ten times to ensure reproducibility and to minimize errors.

3 Results

3.1 Processing

Recording the mass over time continuously, the computer program Labview provides the sets of data points which are further processes in a MATLAB script (still in progress) created by Anton Bijl, member of the Thermal Engineering Group. The MATLAB script generates multiple graphs, examples shown in figures 17, 18 and 19, and outputs the values for reaction rate k, time offset c (starting point of mass decline after sample injection) and ash content a.

Figure 17, 18 and 19 were generated from experiments with torrefied mixed waste wood pellets with size fraction $0 - 200\,\mu$m, at a temperature of 475°C. Figure 17 (a) plots the mass over time curves for all measurements of the series, averaging the beginning (before the first peak) to zero. To plot figure 17 (b), MATLAB detects the first maximum and plots from that point on. T_0, the actual start of the experiment, is thus the time when the first maximum appears. Figure 17 (c) plots the reference curve (in red), which is the curve plotting the mass over time for the inserted nitrogen gas (using gun) only, and the average of all measurements (in green) of one series. For figure 17 (d), the curves are corrected for the mass of nitrogen by subtracting the reference curve from the mass loss curves. This is plotted on the positive y-axis, since this is translated to conversion in the next graph by fitting it to equation 17, therefore normalizing it to one. Smoothing the oscillations, figure 17 (e) shows this fit. The horizontal blue lines mark the fitting range, which is between 0,25 and 0,7. The fitting range makes sure that kinetics are determined from mass loss due to thermal decomposition only.

$$f(t) = 1 - \exp\left(-k \cdot (t - c)\right) \tag{17}$$

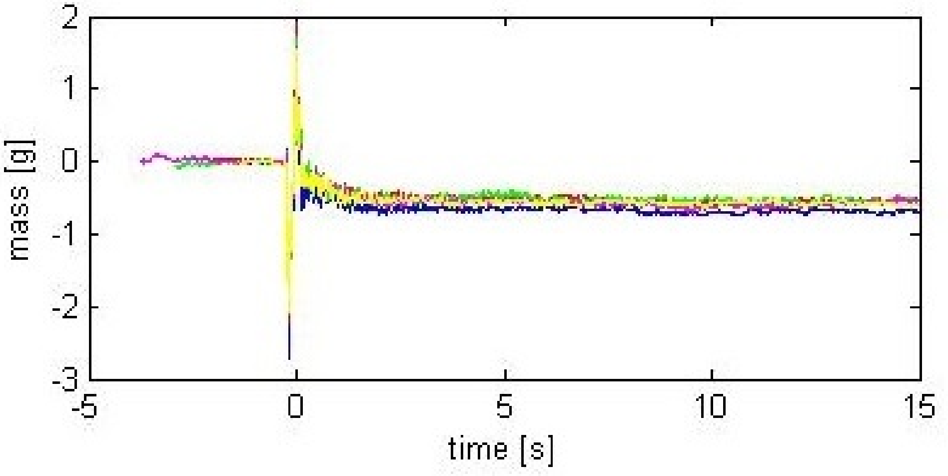

(a) Plot all mass decomposition curves (mass over time); beginning (before first peak) averaged to zero

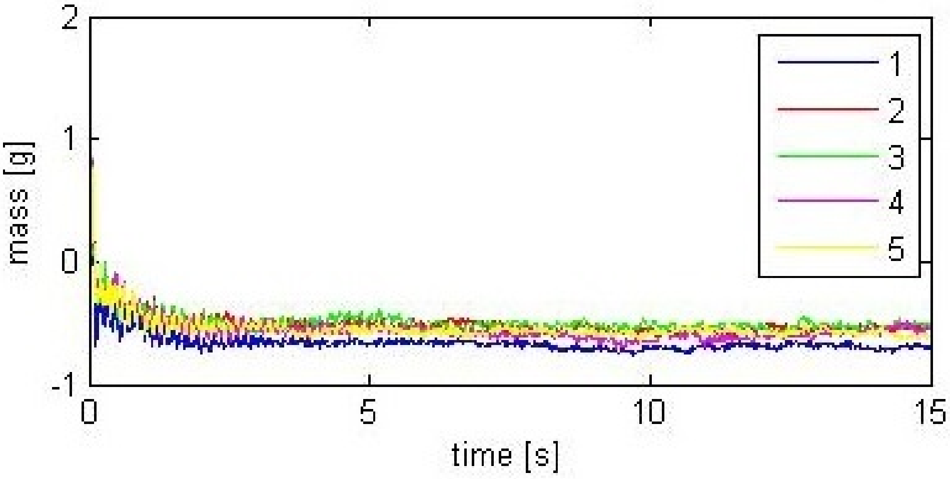

(b) Plot all mass decomposition curves (mass over time) starting at time t_0

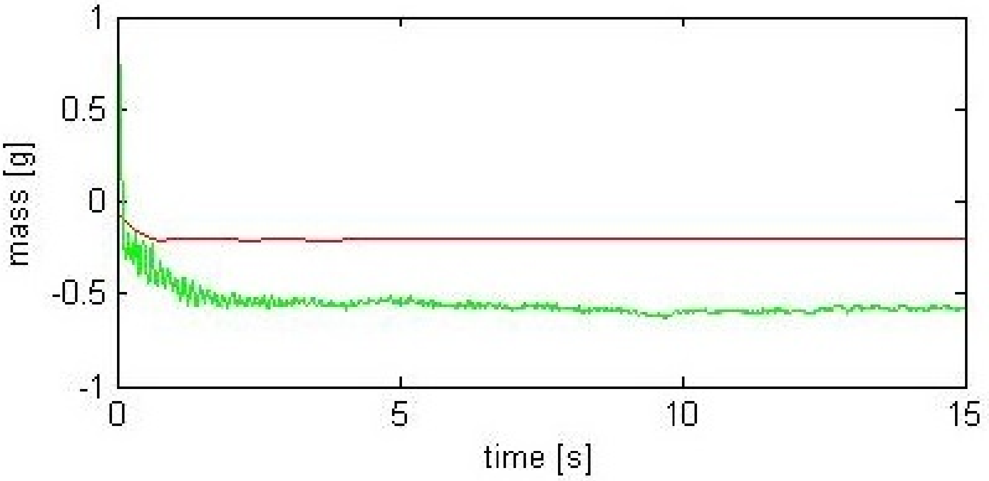

(c) Plot average mass decomposition curves (green) and reference curve (red); mass over time

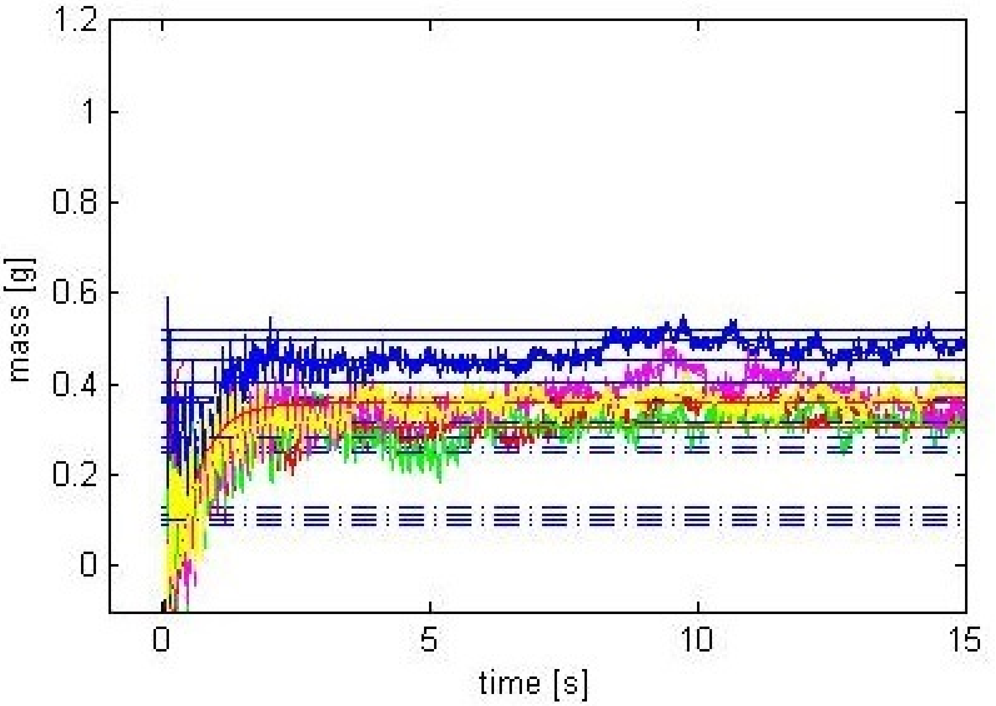

(d) Plot all mass decomposition curves (mass over time) corrected for mass of nitrogen (reference curve)

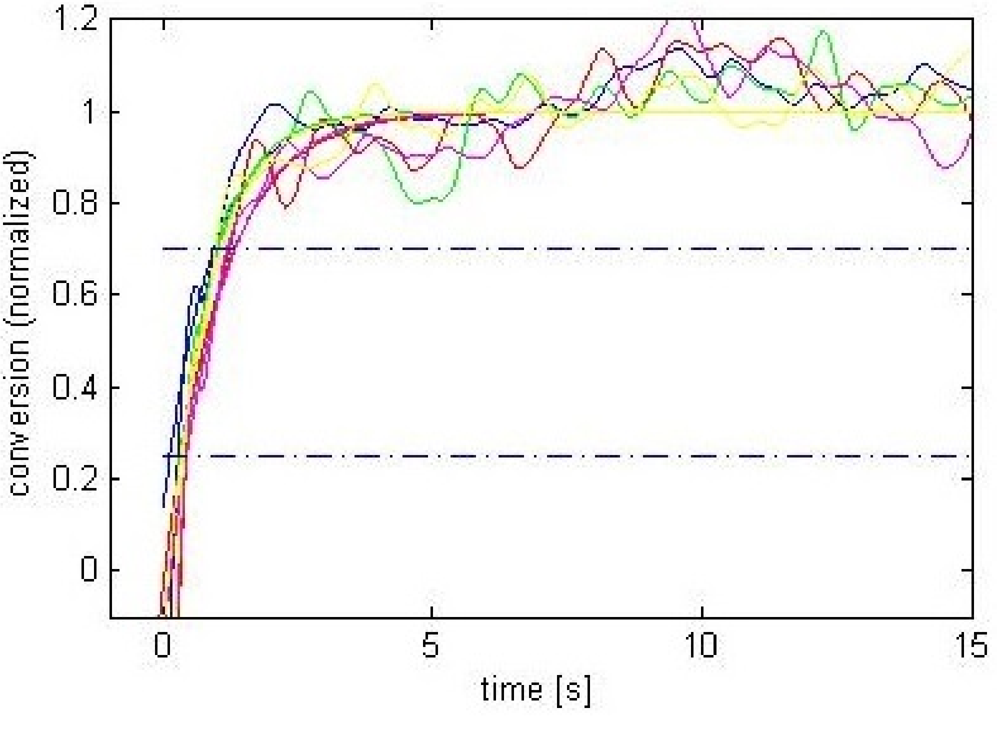

(e) Plot biomass conversion normalized to 1 (conversion over time)

Figure 17: MATLAB output biomass conversion

Figure 18 shows the decomposition of the biomass sample, averaged over all measurements and normalized to -1. Here, 0 means no decomposition has occured and -1 represents full coversion. Figure 19 specifies the k and c values for all measurements as well as their average. K_3 and c_3 are determined from the fit using equation 17 while k_5 and c_5 from fitting with equation

$$\ln(1-y) = -k \cdot (t-c) \tag{18}$$

Since this equation is the same as equation 17, it should yield the same results. This check serves as validation for the correctness of the measurements and MATLAB code. The blue bars are a visualization of the k values (left: k_3 values, right: k_5 values).

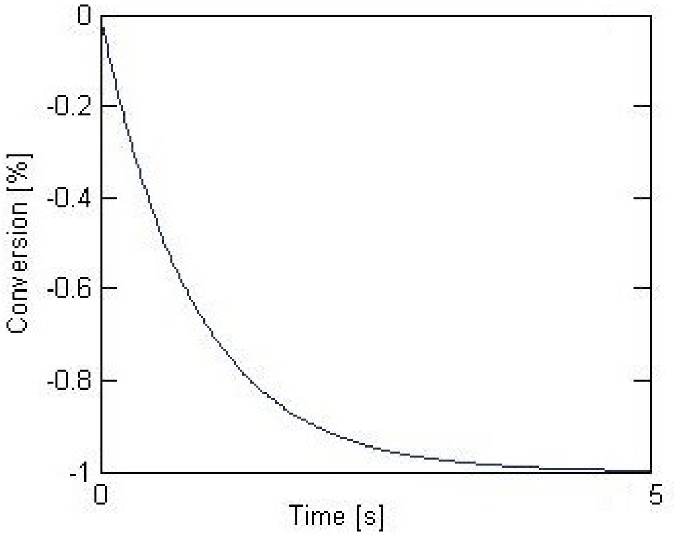

Figure 18: MATLAB output conversion

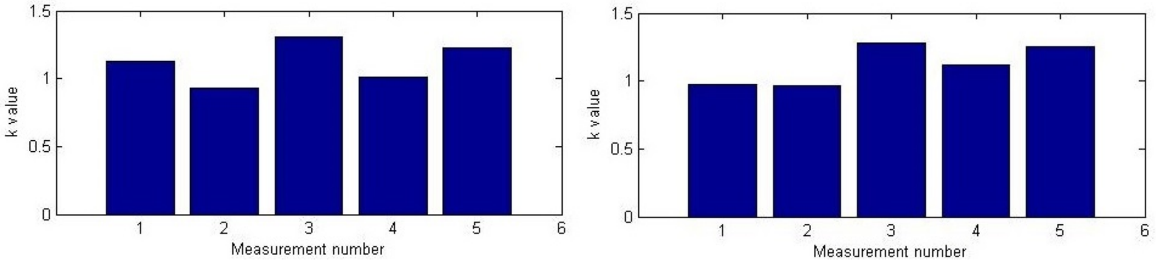

(a) k-value per measurement number

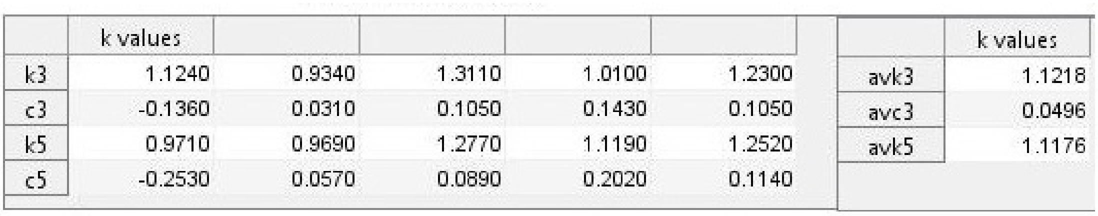

	k values				
k3	1.1240	0.9340	1.3110	1.0100	1.2300
c3	-0.1360	0.0310	0.1050	0.1430	0.1050
k5	0.9710	0.9690	1.2770	1.1190	1.2520
c5	-0.2530	0.0570	0.0890	0.2020	0.1140

	k values
avk3	1.1218
avc3	0.0496
avk5	1.1176

(b) List of all k- and c- values and their average

Figure 19: MATLAB output k- and c-values

The computer program Excel is used to export and further process the k, c and a values provided by MATLAB. For this research, only the k values are of importance. The a and c values are, amongst others, used to determine the quality of a single measurement of a series. The criteria to determine whether a single measurement is of good or bad quality, are listed in 7.1. After omitting odd measurements, the k values of both fittings are averaged, checking whether the difference between them is below 10%.

An Arrhenius plot is created, plotting $\ln(k)$versus $\frac{1}{\mathrm{T}}$ for each particle fraction of each biomass type (raw, torrefied chips and torrefied pellets), by fitting the experimental values to a straight line. From that linear equation, the activation energy E_a and pre-exponential factor A can be determined. While the former is given by the absolute value of the product of slope and universal gas constant ($8.31446\frac{\mathrm{J}}{\mathrm{mol \cdot K}}$), the latter is determined from the exponential of the intercept.

3.2 Analysis and Discussion

3.2.1 Kinetic Parameters

Reaction rates

As explained in 3.1, the reaction rates are processed and compared in Arrhenius graphs. In figures 20, 21 and 22, the Arrhenius plots for raw chips, torrefied pellets and torrefied chips are displayed.

General discussion all Arrhenius plots

The Arrhenius plots fit the reaction rates for the particle distributions 0-200, 200-500 and 500-800 μm for raw chips, torrefied chips and torrefied pellets for 475, 500, 525 and 500°C to a straight line. The x-axis is given by the inverse of temperature (in K) and the y-axis by $\ln(k)$.

The trend for all three material types is that the smallest particles have the largest reaction rate, followed by the medium and large particles. This means that reaction time increases with particle size. For kinetic control, reaction time is not a function of particle size. To determine the maximum particle size, the Biot and Py' numbers are calculated in 3.2.2. In general, each condition contains at least five data points; some not being visible due to overlap with other data points. This is not enough data to draw definite solution but sufficient to see if any trends are developing. The data points in all Arrhenius plots feature a quite big spread, which is a sign for indefinite results. Possible factors are

Moisture content

A moisture content analysis of the material showed that the raw chips have a water content of 4%, the torrefied pellets of 6% and the torrefied chips of 10%. A large moisture content, especially the one of torrefied chips, might be problematic particularly in the beginning of a kinetic reaction. As detected by [PTHW94] , next to temperature, moisture has an impact on the beginning of the reaction. It is assumed that, since water is one of the volatile components in biomass, it will evaporate as soon as the sample is injected into the reactor as the environment is at elevated temperatures. This should result in a larger reaction rate for moisturized material since water evaporates faster than the biomass itself (hemicellulose, cellulose, lignin) decomposes. This hypothesis is tested by re-doing measurements with dried material.

Non-uniform particles

Particle geometries that are non-spherical might be problematic since temperature profiles are more likely to develop. Since the particles of raw and torrefied chips are of cylindrical geometry, this might be a reason for a large data spread for these materials. It is difficult to directly compare the different geometries as this would require a sieving method that allows to create spherical particles from cylindrical ones. However, some qualitative statements can be made by looking at the ratio of volume and area of the two different geometries, included in the Biot and Py' number.

Particle size

In general, it can be seen that the behavior of the reaction rate over time is changing with particle size. More precisely, the reaction rates are decreasing with particle size, meaning that the reaction time increases as particle size increases. This means that not all particle sizes lie within the kinetic regime. As addressed in the chapter 2.1.4 on kinetic regime, particle size has a major influence on whether a reaction is purely kinetics controlled or if external heat transfers have an influence. In order to check for which particles kinetics are still rate determining, a more thorough analysis is provided in the subsection on Biot and Py' numbers below.

Raw chips

In figure 20, the Arrhenius plot for raw chips is shown, including all reaction rates. From this plot it can be seen that the smallest particles show the smallest data spread, indicating that the linear equation is more reliable than for the larger particle sizes.

Table 3 lists the average reaction rates for raw chips of all three size distributions and four temperatures. The overall trend is that, for all particle sizes, the reaction rate increases with temperature. An irregularity can be seen for 0-200 μm when increasing the temperature from 475°C to 500°C, for 200-500 μm when increasing the temperature from 550°C to 550°C and for 500-800 μm when increasing the temperature from 525°C to 550°C. Reasons for this irregularity could be that the last two particle fractions are too large for kinetic control and that, for all size distributions, the particles are of cylindrical geometry. Both reasons result in temperature profiles within the particles. Nevertheless, the trend shows that the reaction time decreases with temperature, thus, the reaction is faster when temperature is higher. This is in line with the expectations formulated in 2.2.

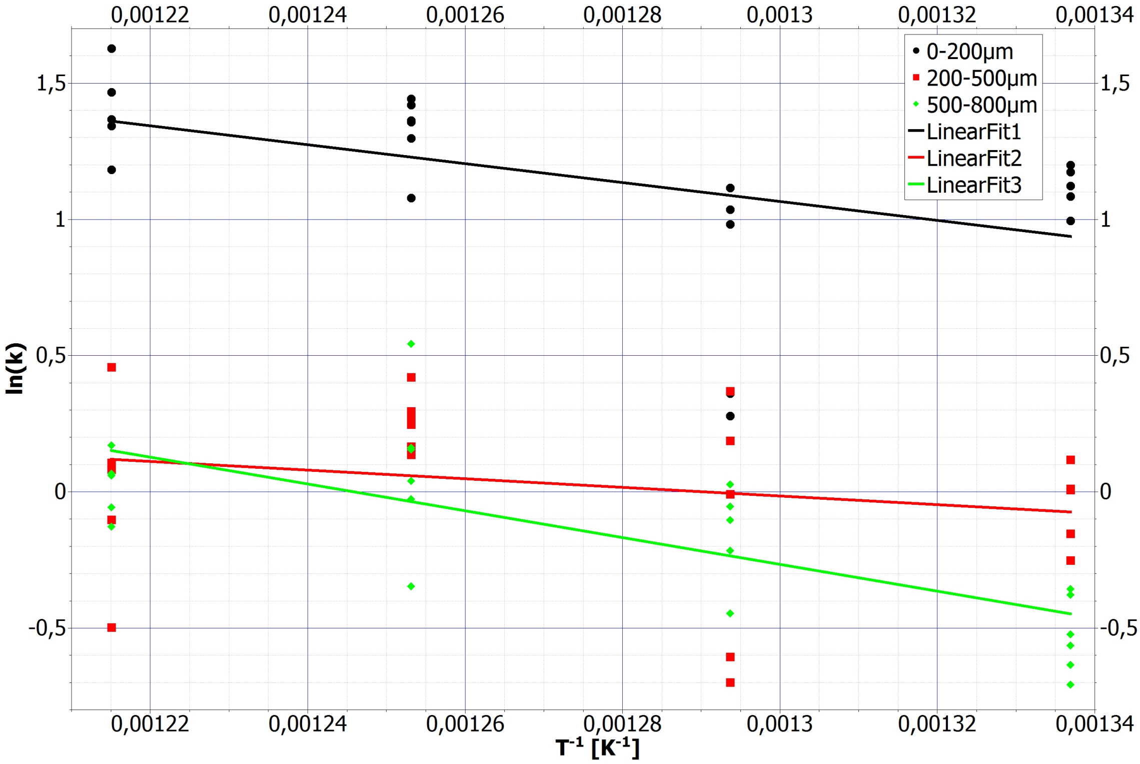

Figure 20: Arrhenius Plot Raw chips, all particle fractions

Table 3: Average reaction rates (in $\frac{1}{s}$) Raw chips

	475°C	500°C	525°C	550°C
0-200 μm	2,99	2,16	3,94	4,15
200-500 μm	0,94	1,05	1,3	1,06
500-800 μm	0,6	0,87	1,19	1,08

Torrefied Pellets

Comparing the data spread of all the Arrhenius plots of all three materials, it can be seen that the torrefied pellets yield the best result, see figure 21. Since the particles are approximately spherical, there should be no heat transfer limitations caused by geometry. The bigger data spread of 200-500 μm and 500-800 μm particles can, again, originate from the particle sizes being out of the kinetic regime. Looking at table 4, the same trend as for the raw chips is visible: When increasing temperature, the reaction rates increase. The only irregularity here are the 500-800 μm particles when the temperature is increased from 525°C to 550°C. This, again, can be caused by the particle sizes lying outside the kinetic regime.

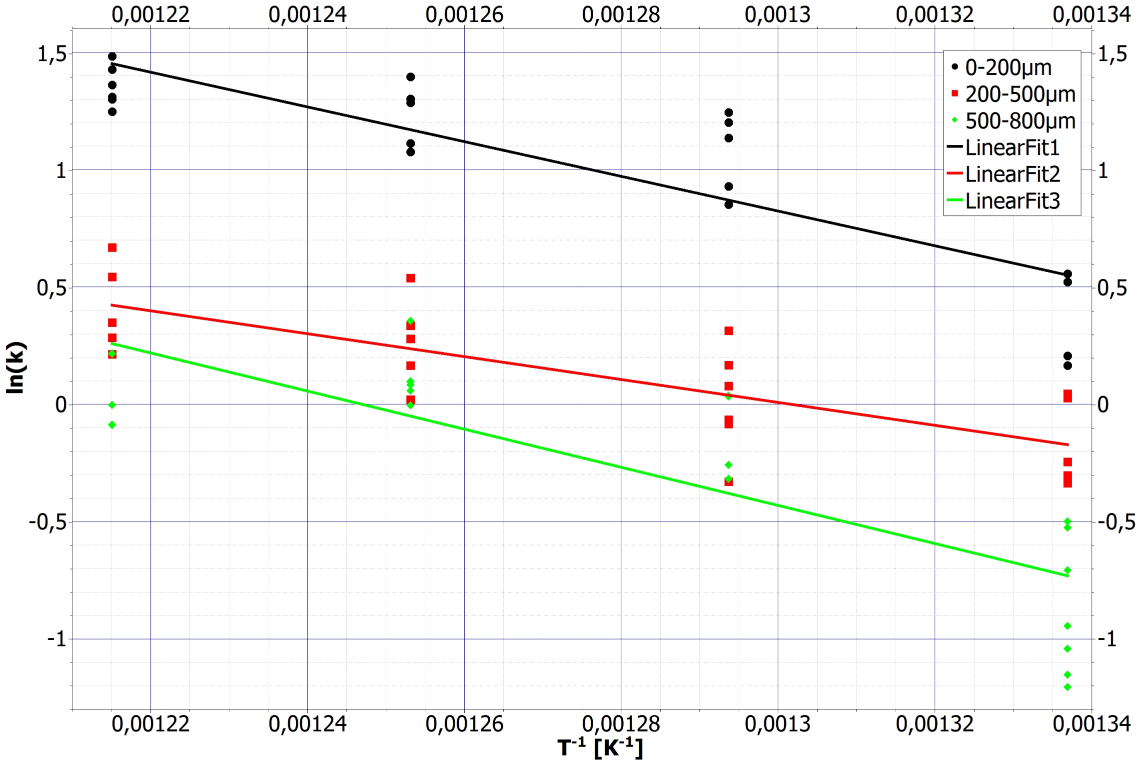

Figure 21: Arrhenius Plot Torrefied Pellets, all particle fractions

Table 4: Average reaction rates (in $\frac{1}{s}$) Torrefied Pellets

	475°C	500°C	525°C	550°C
0-200 μm	1,46	2,96	3,46	3,89
200-500 μm	0,86	1,04	1,33	1,53
500-800 μm	0,44	0,89	1,13	1,06

Torrefied Chips

The Arrhenius plot for torrefied chips, illustrated in figure 22, shows the largest data spread. The material has the highest moisture content (10%), which influences the beginning of the reaction and thus, the overall reaction rate. Further, the particles have a cylindrical geometry, resulting in heat transfer limitations (temperature profiles within the particles). Looking at table 5, the trend is again the same as for raw chips and torrefied pellets: an increase in reaction rate when temperature is increased. The only irregularity here are particles of 500-800 μm when the temperature is increased from 525°C to 550°C. This, again, can be cause of the particle sizes lying outside the kinetic regime.

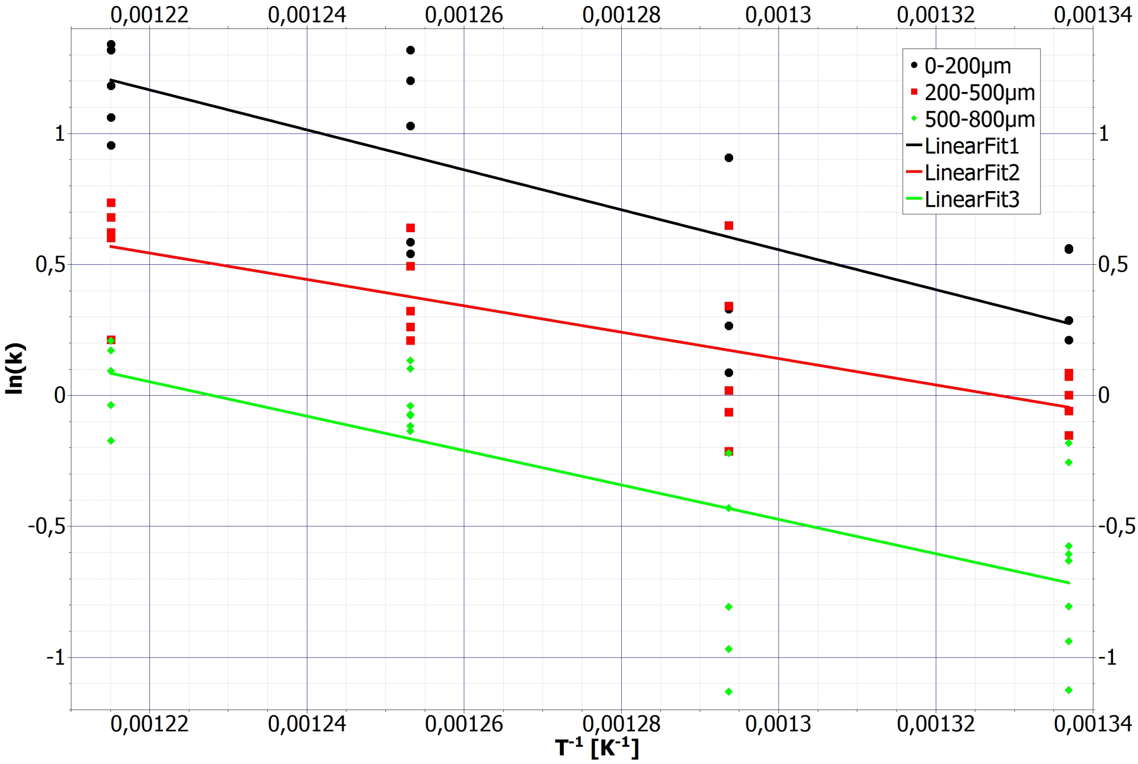

Figure 22: Arrhenius Plot Torrefied Chips, all particle fractions

Table 5: Average reaction rates (in $\frac{1}{s}$) Torrefied Chips

	475°C	500°C	525°C	550°C
0-200 μm	1,43	1,57	2,95	3,26
200-500 μm	0,97	1,22	1,39	1,75
500-800 μm	0,55	0,52	0,98	1,06

Comparison 0-200 μm all materials

The Arrhenius plots for raw material, torrefied pellets and chips show that the particle sizes larger than 200μm seem to be problematic as they might not lie within the kinetic regime any more (further analysis on this part in provided in 3.2.2). For kinetic analysis, a comparison of 0-200μm particles of all materials is made in figure 23. From this plot, the following trends can be seen. First, the reaction rate of the raw chips is larger than the ones of the torrefied materials, which means that raw chips react faster than torrefied material. This is in line with the expectations formulated above. Second, considering both torrefied materials, it can be seen that torrefied pellets experience a larger reaction rate than torrefied chips. This means that densification by pelletization could have an influence on reaction rate of torrefied material by making the reaction faster.

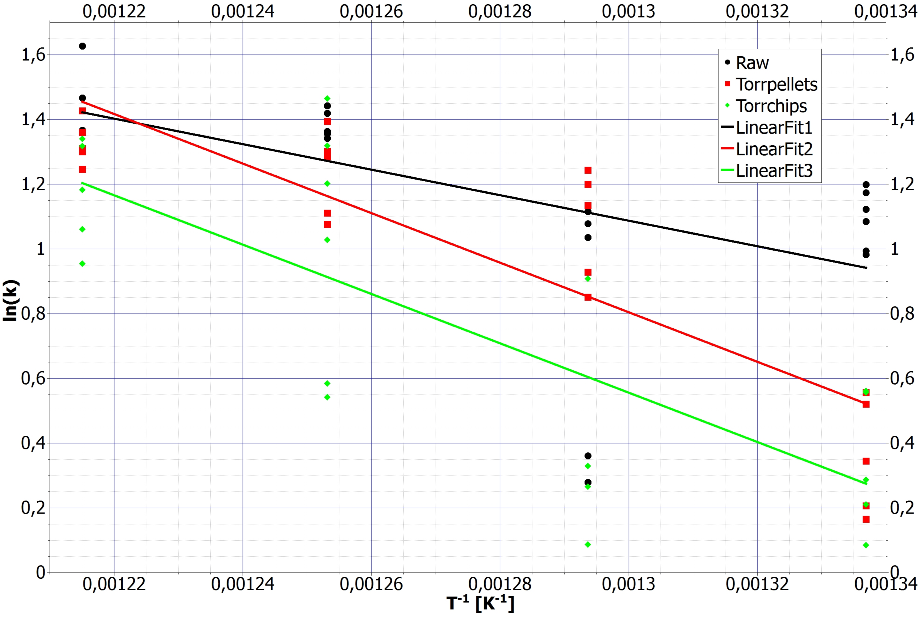

Figure 23: Arrhenius Plot of raw chips, torrefied pellets and torrefied chips of 0-200 μm. Sequence of magnitude of reaction rates: raw chips, torrefied pellets, torrefied chips.

Activation energies and Pre-exponential factors

The activation energies and pre-exponential factors of all materials are listed in tables 6 and 7. Appendix 7.2 presents all values for intercepts and slopes to calculate E_a and A.

The general trend is that raw chips feature a lower activation energy and pre-exponential factor than torrefied material. This is in line with the expectations formulated above. When looking at the torrefied material, the torrefied pellets show a lower activation energy and pre-exponential factor than the chips. However, there is a decrease in activation energy and pre-exponential factor for all three materials from 0-200 μm to 200-500 μm and an increase from 500-800 μm. For pure kinetic control, the activation energies and pre-exponential factors should not change when particle size is varied. Thus, the assumption that particle sizes above 200 μm are not in the kinetic regime any more comes into effect again.

Table 6: Activation Energies

	Activation Energies $\left[\frac{\text{kJ}}{\text{mol}}\right]$		
Particle Size	**Raw chips**	**Torrefied pellets**	**Torrefied chips**
0-200 μm	28,87	61,48	63,39
200-500 μm	13,18	40,66	41,86
500-800 μm	40,89	67,50	54,57

Table 7: Pre-exponential factors

	Pre-exponential Factor $\left[\frac{1}{\text{s}}\right]$		
Particle Size	**Raw chips**	**Torrefied pellets**	**Torrefied chips**
0-200 μm	265	34.066	35.173
200-500 μm	7,74	572	800
500-800 μm	458	24.928	3.164

3.2.2 Kinetic Regime

For kinetic control to be dominant, the Biot number needs to be much smaller than one, preferably below 0.1. When looking at the values presented in table 8, it becomes apparent that only the smallest particles sizes can be considered. Here, the torrefied pellets give the smallest Biot numbers (0,092). The smallest particles of the raw and torrefied chips have a maximum of 0,125 as Biot number, which is still acceptable. Any particle size above yields a higher Biot number.

A further indication for kinetic control is the Py' number, which needs to be much larger than one. The smallest particle sizes of all materials yield the best results. The raw and torrefied chips produce a better result as they feature a larger Py' number than the torrefied pellets.

From the indications for kinetic control it can be concluded that the maximum particle size that can be used for kinetic measurements is 200 μm for all material types. In that way, the heat conduction within the particle is much faster than heat convection to the particle. This heat conduction is faster for torrefied pellets than for raw and torrefied chips. For the aforesaid particle size it also applies that heat convection to the particle is much faster than the chemical reaction taking place. This heat convection is faster for raw and torrefied chips than for torrefied pellets.

When looking at the surface-to-volume ratio of the two geometries, these conclusions make sense. For a sphere, the surface-to-volume ratio is larger than for a cylinder. This means that particles of spherical geometry react faster than particles of cylindrical geometry since there is more surface area available to react. This only applies if the other properties are alike. Therefore, only the torrefied pellets and chips can be compared using this criterion as their elemental analysis is more similar than that of raw wood. Table 16 in 7.3 lists the elemental analysis. Since the torrefied pellets are of spherical geometry, they should react faster than the cylindrical torrefied chips. This is in line with the Arrhenius plot, shown in figure 23, and hence the reaction rates. However, at this point it becomes difficult to determine whether the difference in reaction rate, activation energy and pre-exponential factor of torrefied chips and pellets results from densification or from the difference in geometry. To examine this, experiments should be conducted keeping one of the parameters constant. By keeping the geometry constant, the influence of densification can be determine while keeping the pre-treatment constant allows to check on the influence of geometry.

Table 8: Biot and Py' numbers

			Biot number		**Py' number**	
	Assumption	Particle size	**Min**	**Max**	**Min**	**Max**
Raw chips	Cylindrical particles	0-200 μm	0	0,125	0	57,62
		200-500 μm	0,125	0,313	57,62	23,05
		500-800 μm	0,313	0,5	23,05	14,40
Torrefied pellets	Spherical particles	0-200 μm	0	0,092	0	48,25
		200-500 μm	0,092	0,229	48,25	19,3
		500-800 μm	0,229	0,367	19,30	12,06
Torrefied chips	Cylindrical particles	0-200 μm	0	0,125	0	57,21
		200-500 μm	0,125	0,313	57,21	22,88
		500-800 μm	0,313	0,5	22,88	14,30

3.2.3 Influence of Moisture Content

In order to test the assumption that moisture content has an influence on the reaction, measurements with dried biomass of all three material types have been done. The results are shown in figure 24. All three Arrhenius plots show the trend that moisture has an impact on the reaction rate: dried material features a lower reaction rate than moisturized material. This means that dried material reacts slower than wet material. Table 9 lists the average reaction rates of all three materials of size 0-200μm.

Table 10 lists the activation energies and pre-exponential factors of moisturized and dried material of all three material typed of 0-200μm. From the table it can be seen that both activation energy and pre-exponential factor change when feeding dried material. However, there is no consistency in whether the parameters decrease or increase. For moisturized raw wood and torrefied chips, the activation energy and pre-exponential factor are lower than for the dried material. For torrefied pellets, the activation energy and pre-exponential factor are higher for moisturized than for dried material.

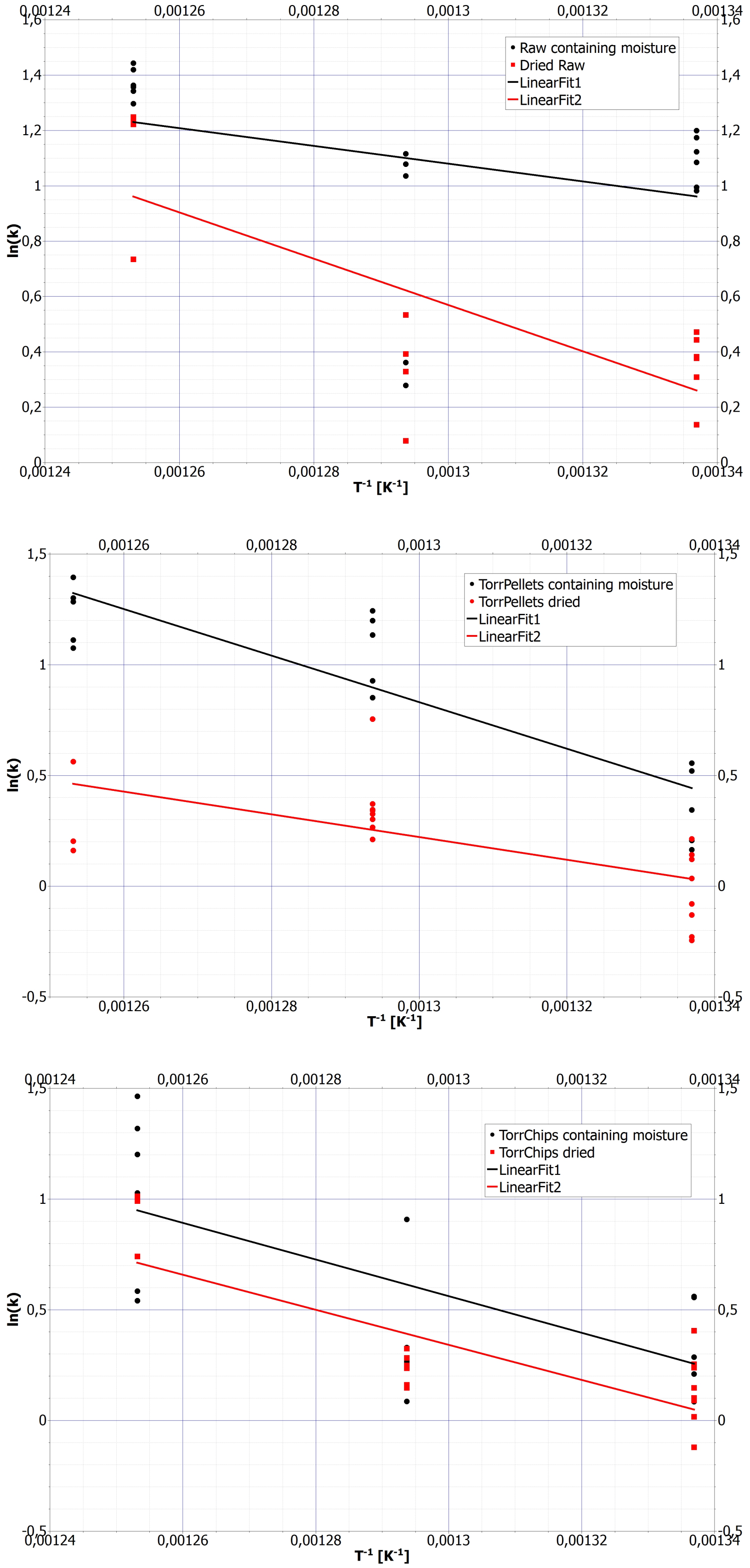

Figure 24: Comparison of moisturized and dried biomass of particle size 0-200μm. *Top*: Raw chips, *middle*: Torrefied pellets, *bottom*: Torrefied chips

Table 9: Comparison reaction rates (in $\frac{1}{s}$) of moisturized and dried material of all three material types of size fraction 0-200μm

	475°C	500°C	525°C
Moisturized Raw	2,99	2,16	3,94
Dried Raw	1,43	1,42	3,1
Moisturized Torrefied Pellets	1,46	2,96	3,89
Dried Torrefied Pellets	0,99	1,46	1,39
Moisturized Torrefied Chips	1,43	1,57	2,95
Dried Torrefied Chips	1,14	1,25	2,52

Table 10: Activation Energies and Pre-exponential factors of dried and moisturized materials of particle size 0-200μm

Material	**Activation Energy** [$\frac{\mathrm{kJ}}{\mathrm{g}}$]	**Pre-exponential factor** [$\frac{1}{\mathrm{s}}$]
Moisturized Raw wood	28,87	265
Dried Raw wood	69,53	92.974
Moisturized Torrefied Pellets	61,48	34.066
Dried Torrefied Pellets	42,64	981,46
Moisturized Torrefied Chips	63,39	35.173
Dried Torrefied Chips	65,81	41.397

4 Conclusion

The overall goal of this research was to determine the pyrolysis reaction kinetics of raw and torrefied biomass in order to create a kinetic model of biomass particles. The kinetic model includes reaction rate, activation energy and pre-exponential factor. It was further desired to investigate how torrefaction changes the conversion time of biomass, which is essential information for reactor design.

To make statements about the kinetic parameters, heat transfer limitations and temperature profiles withinn the biomass particles are probibited. Therefore, particle size is the limiting parameter. Results show that a maximum particle size of 200 μm for all three biomass types (raw chips, torrefied pellets and torrefied chips) can be used in the cyclonic TGA reactor.

For 0-200 μm particles, the trends show that reaction rate, activation energy and pre-exponential factor of raw and torrefied biomass are different. The reaction rate of raw chips is larger than those of the torrefied materials, indicating a faster reaction of the former. The activation energy is lower for raw chips than for the torrefied materials. This means that a lower amount of energy is necessary for the raw chips to start reacting than for torrefied material. Both trends are in line with the formulated expectations.

It was further aimed at investigating the influence of densification of torrefied chips on the kinetic parameters. The trends show that densification has an impact on reaction rate, activation energy and pre-exponential factor as torrefied pellets yield different results than torrefied chips. The trend is that torrefied pellets have a larger reaction rate, thus, react faster, than torrefied chips. The activation energy and pre-exponential factor are lower for torrefied pellets than for torrefied chips.

In the course of this research, it has been sensed that the moisture content of the material might have an influence on the kinetic behavior of all three materials. Comparison to measurements with dried biomass show that moisture content increases the reaction rates for all three materials. The activation energy and pre-exponential factor are increased when drying the raw and torrefied chips and decreased when drying the torrefied pellets.

5 Recommendations

No definite conclusion about the impact of densification could be drawn since the difference in kinetic parameters could also come from the fact that the particles are of different geometry. Therefore, it is recommended to investigate the influence of particle geometries on the reaction.

Since the degree of torrefaction can be very different, it is advised to check how this influences the reaction kinetics. This could be done by self-torrefying material at different temperatures and residence times. Here, different feedstocks should be used as well to see if torrefaction severity has a similar impact on different material types. It is expected that reaction rate decreases with increasing torrefaction severity. The exact values are expected to differ for different feedstocks due to diverse composition of biomass, for example of hard and soft wood.

In order to get a deeper insight into the kinetic regime, the particle range of 0-200 μm should be further divided into smaller fractions to see if reaction time still changes. Also, the flow rates of nitrogen could be varied as this has direct influence on heat transfer limitations: these decrease when the flow rate is increased. Some measurements with varying gas flow rates were conducted by [BB07], yet not for torrefied material.

In order to understand why certain measurements go wrong, the mass of the produced bio-oil could be measured. It is expected that for odd experiments, the bio-oil formation is problematic.

6 Acknowledgements

First and foremost, I would like to thank my supervisor Alexander Louwes. I am thankful for your support and guidance throughout my entire bachelor assignment. It was a pleasure to have a cooperative and open minded supervisor who always had an open door for discussions and modifications. I would also like to show gratitude to the chairperson of my examination committe, Dr. Eddy Bramer and to the external member, Dr. Arie van Houselt. I am thankful that Dr. Eddy Bramer, who was one of my professors in the course ”Energy from Biomass”, raised my interest in this bachelor assignment. I would also like to thank Dr. Arie van Houselt for being a great help in kinetics related questions.

It was a pleasure to be part of the Thermal Engineering group, which is a very enjoyable, communicative and open minded team. I wish all group members great success with future research.

References

[BB07] Bramer, E. A. ; Brem, G.: New thermogravimetric vortex reactor for the determination of the primary decomposition rate of biomass at fast pyrolysis conditions. (2007)

[Bra13] Bramer, E. A.: *Pyrolysis of Biomass.* December 2013. – Lecture No. 6 Energy from Biomass course, University of Twente

[Bri12] Bridgwater, A. V.: Review of fast pyrolysis of biomass and product upgrading. In: *Biomass and Bioenergy* 38 (2012), S. 68–94

[CG11] Cengel, Y.A. ; Ghajar, A.J.: *Heat and Mass Transfer - Fundamentals and Applications.* 4. Mc Graw Hill, 2011. – page 228

[DB08] Di Blasi, C.: Modeling chemical and physical processes of wood and biomass pyrolysis. In: *Progress in Energy and Combustion Science.* 34(1) (2008), S. 47–90

[Ker13] Kersten, S.R.A.: *Introduction to biomass, conversion and biorefinery.* November 2013. – Lecture No.2 Energy from biomass course, University of Twente

[MPTP12] Meng, J. ; Park, J. ; Tilotta, D. ; Park, S.: The effect of torrefaction on the chemistry of fast-pyrolysis bio-oil. In: *Bioresource technology* 111 (2012), S. 439–446

[Nac] `http://www.ugent.be`

[NRVP12] Nachenius, R. ; Ronsse, F. ; Venderbosch, R. ; Prins, W.: Biomass pyrolysis. In: *Chemical Engineering for Renewables Conversion.* (2012), S. 75–139

[PBVG09] Prime, R. B. ; Bair, H. E. ; Vyazovkin, S. ; Gallagher, P. K. ; Menczel, J.D. (Hrsg.) ; Prime, R.B. (Hrsg.): *Thermogravimetric Analysis (TGA). Thermal Analysis of Polymers, Fundamentals and Applications, 241-317.* Wiley, 2009

[PPJ06] Prins, M. J. ; Ptasinski, K. J. ; Janssen, F. J.: Torrefaction of wood: Part 1. Weight loss kinetics. In: *Journal of Analytical and Applied Pyrolysis.* 77(1) (2006), S. 28–34

[PTHW94] Peterson, B. I. ; Tong, C. H. ; Ho, C. T. ; Welt, B. A.: Effect of moisture content on Maillard browning kinetics of a model system during microwave heating. In: *Journal of Agricultural and Food Chemistry* 42(9) (1994), S. 1884–1887

[SGKP11] Stelt, M. J. C. d. ; Gerhauser, H. ; Kiel, J. H. A. ; Ptasinski, K. J.: Biomass upgrading by torrefaction for the production of biofuels: A review. In: *Biomass and Bioenergy* 35(9) (2011), S. 3748–3762

[Vis05] Vissers, Roy: *Two phase flow in a cyclone reactor*, University of Twente, Enschede, Diplomarbeit, 2005

[WCL11] White, J. E. ; Catallo, W. J. ; Legendre, B. L.: Biomass pyrolysis kinetics: A comparative critical review with relevant agricultural residue case studies. In: *Journal of Analytical and Applied Pyrolysis* 91(1) (2011), S. 1–33

[ZZC+13] Zheng, A. ; Zhao, Z. ; Chang, S. ; Huang, Z. ; Wang, X. ; He, F. ; Li, H.: Effect of torrefaction on structure and fast pyrolysis behavior of corncobs. In: *Bioresource technology* 128 (2013), S. 370–377

7 Appendix

7.1 Indications for Quality of Experiment

In order to see which experiments were erroneous, statistical outliers were determined and ”visual inspection’ applied.

Statistical Outliers

An outliner is a candidate for omission from the data set. The procedure for determining statistical outliers is as follows.

- determine the mean ”Q2”
- determine data point ”Q2” below which 25% of the data sits
- determine data point ”Q3” above which 75% of data sits
- determine ”interquartile range (IR)”, which sets the boundaries for non-outlier points in data set: IR=Q3-Q1
- determine boundaries for ”inner fences”, which yield minor outliers:

  $Q1 - IR^2$

  $Q3 + IR^2$

- determine boundaries for ”outer fences”, which yield major outlinerss

  $Q1 - 2 \cdot IR^2$

  $Q3 + 2 \cdot IR^2$

Visual Inspection

MATLAB output

Figures 25, 26 and 27 show the graphs of torrefied 0-200 μm mixed waste wood fed to the cyclonic TGA at 475 °C. Here, all the measurements are included while in figures 17, 18 and 19 the odd ones are omitted. The qualitative criteria for visual inspection are as follows

- In figure 25 (b) and (c), check if the curves are approximately on top of each other. In this case, the blue (1) and green (3) curves lie a lot higher than the others.
- In figure 25 (e), the point of 75% conversion is of importance. The range in which the curves hit that point, should be small enough as the biomass samples should convert equally fast. As one can see, the pink curve (4) is off. The green (3) and black (6 or 8) seem to be problematic as well.

- In figure 27 (a), a big difference in k values is visible. The ones that do not fit with the others are problematic. Especially measurement numbers 1, 3, 4 and 6 are much different.
- The table in figure 27 (b) lists the c values. Here, the ones of measurements 2 and 4 are negative, which is problematic. A negative c value means that the measurement has started before the actual start of the experiment. Also, c value number 6 is much higher than the others, which makes it a possible measurement for omission.
- Table 11 lists the a values for all measurements. For measurement number 1 and 3, the a value is larger than the original sample weight of 0.5 g. This means that weight should have been gained during the experiment, which is impossible. As the a value of measurement number 2 is close to 0.5, it is problematic as well.
- Taking all the criteria into consideration, it becomes apparent that measurement numbers 1, 3, 4 and 6 should be omitted.

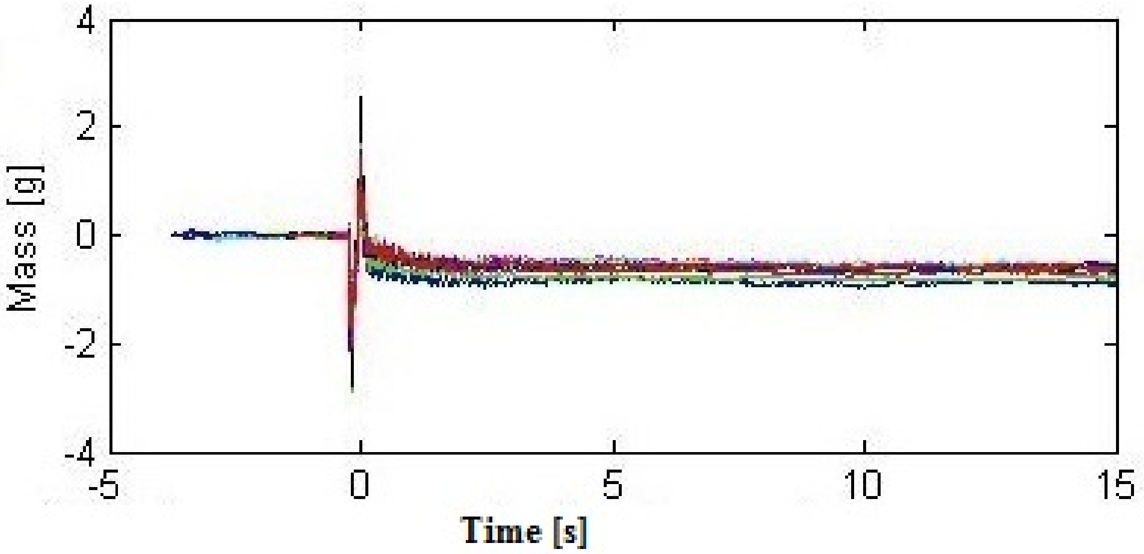

(a) Plot all mass decomposition curves (mass over time); beginning (before first peak) averaged to zero

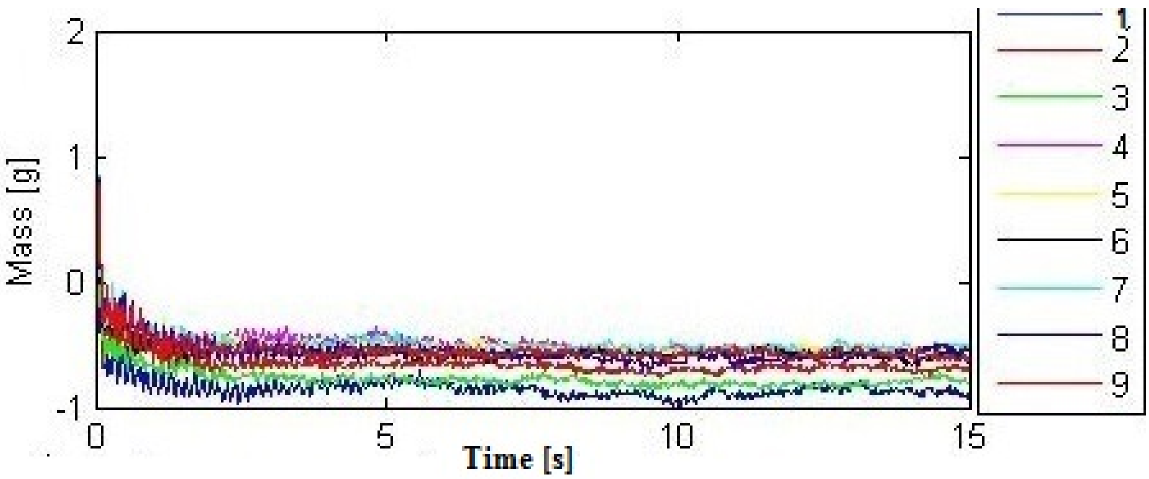

(b) Plot all mass decomposition curves (mass over time) starting at time t_0

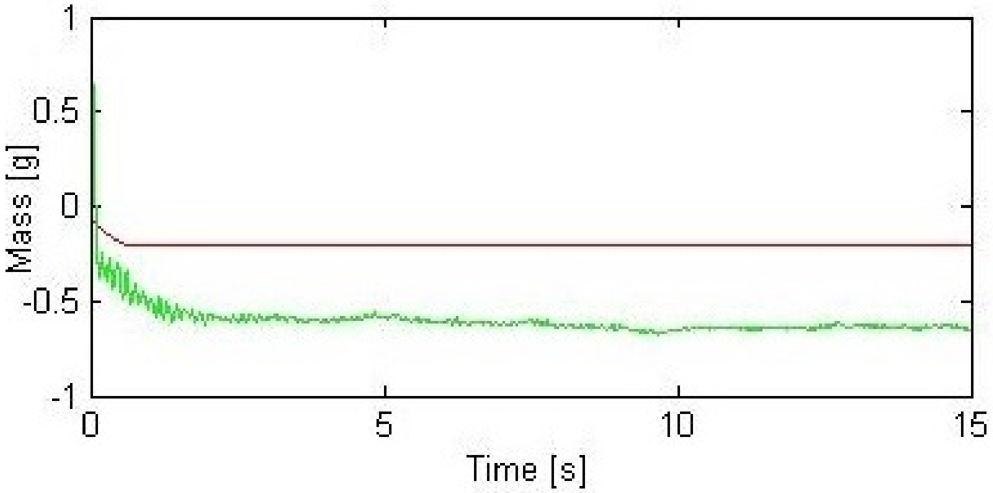

(c) Plot average mass decomposition curves (green) and reference curve (red); mass over time

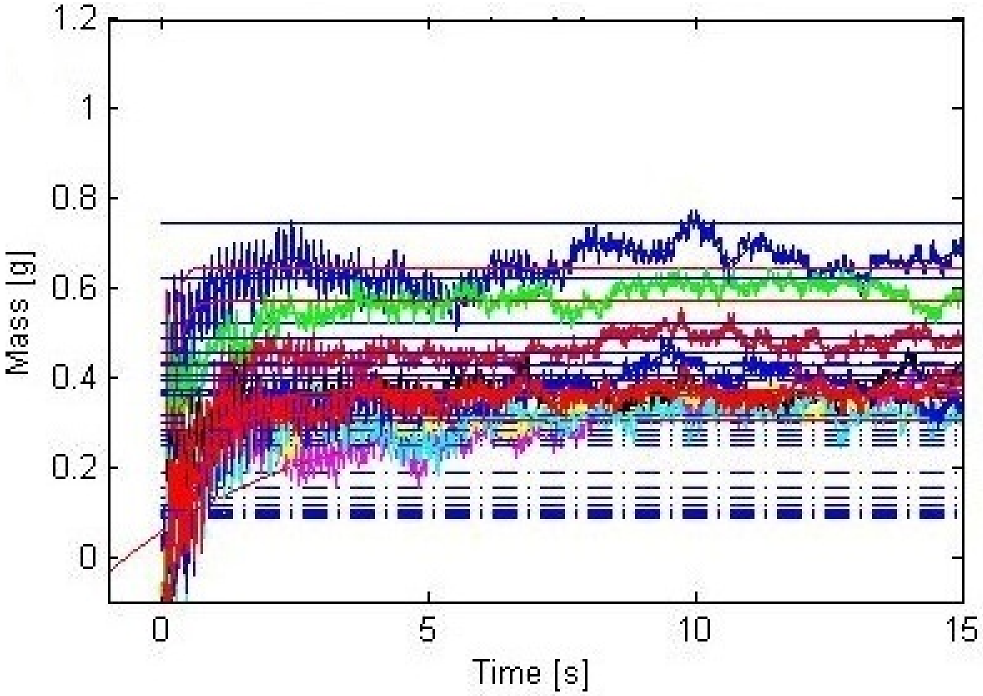

(d) Plot all mass decomposition curves (mass over time) corrected for mass of nitrogen (reference curve)

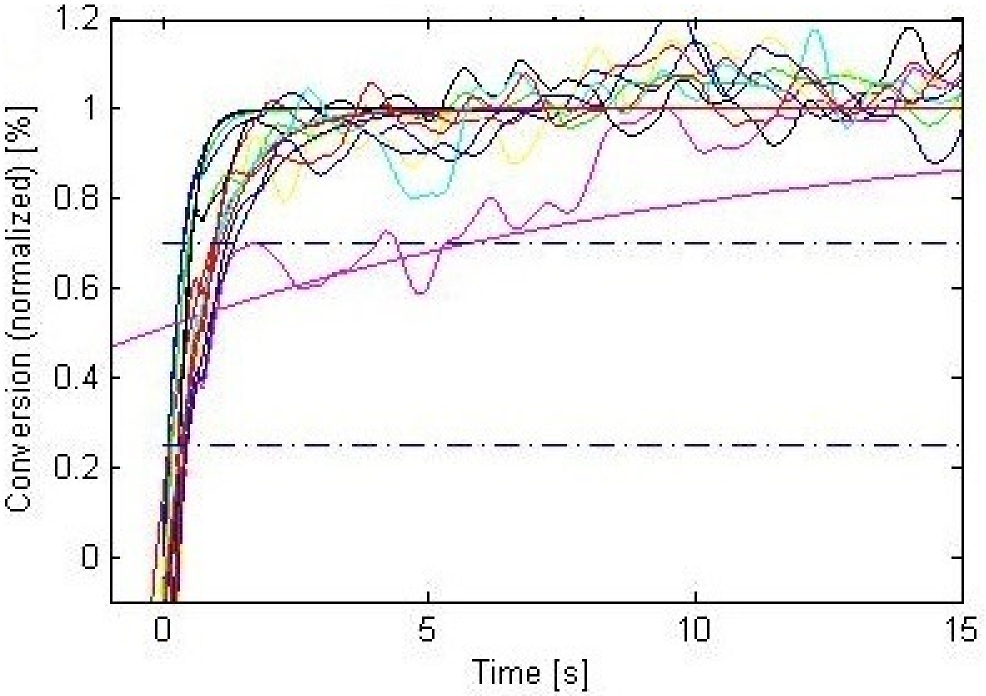

(e) Plot biomass conversion normalized to 1 (conversion over time)

Figure 25: MATLAB output biomass conversion including all measurements

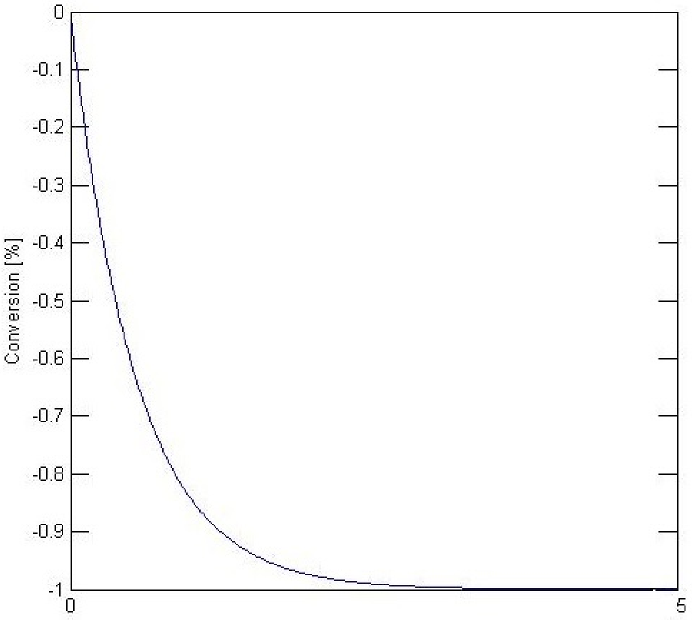

Figure 26: MATLAB output conversion

Table 11: a values

Measurement number	1	2	3	4	5	6	7	8	9
a value	0,647	0,456	0,571	0,359	0,318	0,36	0,304	0,372	0,358

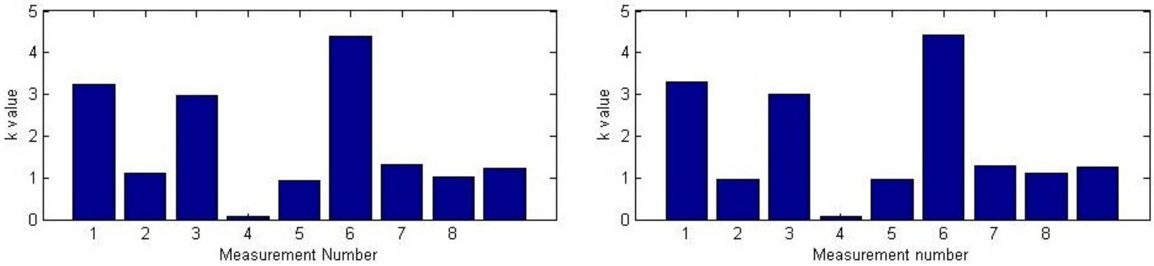

(a) k-value per measurement number

	k values								
k3	3.2420	1.1240	2.9820	0.0850	0.9340	4.3940	1.3110	1.0100	1.2300
c3	0.0140	-0.1360	0.0710	-8.4020	0.0310	0.2500	0.1050	0.1430	0.1050
k5	3.3020	0.9710	2.9930	0.0600	0.9690	4.4110	1.2770	1.1190	1.2520
c5	0.0180	-0.2530	0.0710	-13.3930	0.0570	0.2510	0.0890	0.2020	0.1140

	k values
avk3	1.8124
avc3	-0.8688
avk5	1.8171

(b) List of all k- and c- values and their average

Figure 27: MATLAB output k- and c-values

Mass decomposition

During the measurements, qualitative statements about the quality of an experiment can be made as well. First, the mass decomposition graph, an example shown in figure 15, should not show more than one peak. Further, after the experiment, it is problematic if a lot of biomass is blown out of the reactor during cleaning. This means that biomass has not fully reacted.

7.2 Linear Equations Arrhenius Plots

The linear equations are of the general form

$$y = m \cdot x + c \tag{19}$$

Table 12 - 15 show the constants for all materials used.

Particle size	m	c
0-200 μm	-3.472	5,58
200-500 μm	-1.586	2,05
500-800 μm	-4.918	6,13

Table 12: Moisturized raw

Particle size	m	c
0-200 μm	-7.624	10,47
200-500 μm	-5.034	6,69
500-800 μm	-6.564	8,06

Table 13: Moisturized Torrefied pellets

Particle size	m	c
0-200 μm	-7.624	10,47
200-500 μm	-5.034	6,69
500-800 μm	-6.564	8,06

Table 14: Moisturized Torrefied chips

Particle size	m	c
Raw	-8.362	11,44
Torrefied pellets	-5.128	6,89
Torrefied chips	-7.915	10,63

Table 15: Dried material 0-200 μm

7.3 Elemental Analysis

Table 16 shows the elemental analysis for raw chips, torrefied pellets and torrefied chips.

Table 16: Elemental analysis

Material	N [%]	C [%]	H [%]	Ash [%]	Water [%]	O (by difference)[%]	O/C ratio
Raw chips	0,78	48,42	6,16	7,96	3,69	32,53	0,67
Torrefied pellets	0,41	49,46	5,7	3,61	6,45	33,56	0,68
Torrefied chips	0,44	47,29	5,54	4,29	10,11	31,07	0,66